Zoology 153 (2022) 126027

Contents lists available at ScienceDirect

Zoology

journal homepage: www.elsevier.com/locate/zool

Form and function of the mantle edge in Protobranchia (Mollusca: Bivalvia)

Carmen Salas [a,b,*], Juan de Dios Bueno-Pérez [c], Juan Félix López-Téllez [d], Antonio G. Checa [e,f]

[a] Departamento de Biología Animal, Facultad de Ciencias, Universidad de Málaga, 29071 Málaga, Spain
[b] Instituto de Biotecnología y Desarrollo Azul (IBYDA), Universidad de Málaga, Centro de Experimentación Grice-Hutchinson, 29004 Málaga, Spain
[c] Centro de Instrumentación Científica, Universidad de Granada, 18071 Granada, Spain
[d] Instituto de Investigación Biomédica de Málaga y Plataforma en Nanomedicina-IBIMA Plataforma BIONAND, 29590 Campanillas, Málaga
[e] Departamento de Estratigrafía y Paleontología, Facultad de Ciencias, Universidad de Granada, 18071 Granada, Spain
[f] Instituto Andaluz de Ciencias de la Tierra, CSIC-Universidad de Granada, 18100 Armilla, Spain

ARTICLE INFO

Keywords:
Sarepta
Acila
Nucula
Nuculana
Lembulus
Solemya
Periostracum
Valve crenulations
Ennucula

ABSTRACT

We analyzed, by optical and transmission electron microscopy, the morphology and function of the mantle edge, including the formation of the periostracum, of ten species of protobranchs. Five species from the order Nuculida, four species from the order Nuculanida and one species from the order Solemyida were studied. A second outer fold, which seems to function as a template for the internal marginal crenulations of the valves, is present in the crenulated species of *Nucula*. The minute non-crenulated *Ennucula aegeensis* shows the glandular basal cells displaced toward the periostracal groove, resembling a minute additional fold between the outer and middle folds. Intense secretion of glycocalyx, together with active uptake of particles, have been observed in the inner epithelium of the middle mantle fold and the whole epithelium of the inner mantle fold in all the studied species. Contrary to the rest of the bivalves, all the protobranchs analyzed have two basal cells involved in the formation of the external nanometric pellicle of the periostracum, a character that would support the monophyly of protobranchs. A three-layered pattern is the general rule for the periostracum in protobranchs, like for other bivalves. The presence of pouches of translucent layer inside the tanned dark layer under periostracal folds is characteristic of the species with a folded periostracum; its function is unclear but could give flexibility to the periostracum. The non-nacreous internal shell layer and the presence of translucent pouches under periostracal folds in *Sarepta speciosa* resemble those found in nuculanids. However, the free periostracum is rather similar to those of *N. hanleyi* and *E. aegeensis,* with a continuous vesicular layer. All the latter supports the inclusion of *Sarepta* in the order Nuculanida but could indicate either a basal lineage or that the translucent vesicular layer is an adaptive trait.

1. Introduction

The mantle, the dorsal integument of the molluscs, is responsible for the secretion of the shell or calcareous spicules in this phylum. The shell begins at the mantle edge, where the periostracum and outer layer of the shell originated, while the overall mantle epithelium secretes the inner shell layer (Stasek and McWilliams, 1973; Ponder et al., 2019). In bivalves, the only contact with the environment is the mantle edge, for which sensorial organs such as eyes, tentacles, or sensorial cells can be present (Audino et al., 2015). The mantle margin of bivalves is therefore deeply associated with the animal's mode of life (Yonge, 1983; Audino and Marian, 2016; Audino and Marian, 2018).

The mantle edges of bivalves show a diversity of forms but in general, they have three mantle folds, of which the outer fold is involved with the shell formation, the middle fold presents sensorial cells and organs, and the muscular inner fold controls the water flow through the pallial cavity (Yonge, 1983; Morse and Zardus, 1997). However, this general pattern presents morphological variations among the clades of Bivalvia, such as the Pteriomorphia, in which the mantle margin diversification could be correlated with transitions in pteriomorphian life habits (Audino and Marian, 2016). The mantle margin, therefore, represents a good model to study convergent evolution, due to its strong association with habitat use and lineage diversification (Audino and Marian, 2016; Audino et al., 2020).

The periostracum, the waterproof outermost layer of bivalve shells, begins at the bottom of the periostracal groove, which is located

* Corresponding author at: Departamento de Biología Animal, Facultad de Ciencias, Universidad de Málaga, 29071 Málaga, Spain.
E-mail addresses: casanova@uma.es (C. Salas), juandeb@ugr.es (J.D. Bueno-Pérez), juanfelix.lopez@ibima.eu (J.F. López-Téllez), acheca@ugr.es (A.G. Checa).

https://doi.org/10.1016/j.zool.2022.126027
Received 23 January 2022; Received in revised form 2 May 2022; Accepted 24 June 2022
Available online 28 June 2022

between the outer and middle folds. It has two main functions: (a) to supply the matrix for the deposition of calcium carbonate crystals in the mineralization process of the shell and (b) to protect the shell from the environment. The knowledge of the origin of the periostracum at the cellular level is still scarce (Checa and Salas, 2017). Independently of its function, the periostracum can also provide useful characters for systematics (Salas et al., 2012, for Astartidae).

The subclass Protobranchia is one of the less well known bivalve clades, probably because most of its ca. 750 species are inhabitants of the deep sea (Allen and Sanders, 1996; Zardus, 2002; Zardus et al., 2006). The highest level of genetic and morphological divergence among protobranchs is found in the bathyal zone, suggesting that the bathyal may be a more active area of species formation than the abyssal zone, probably due to its strong biotic and abiotic heterogeneity (Etter et al., 2005). Low genetic divergence across thousands of kilometers of horizontal distance has been observed among several Atlantic deep-sea protobranchs (Zardus et al., 2006; Etter et al., 2011; Jennings et al., 2013). Ecological speciation probably plays a more prominent role in diversification than previously thought, particularly in marine ecosystems where dispersal potential is great and where there are few obvious barriers to gene flow. This seems to be especially true in the deep sea where allopatric speciation looks insufficient to account for the rich and largely endemic fauna (Jennings et al., 2013).

Pelseneer (1891) established the order Protobranchia from the examination of structures of species of *Nucula*, *Leda* (accepted as *Nuculana*), *Yoldia,* and *Solenomya* (accepted as *Solemya*), regarding them as a primitive group within the Lamellibranchia. The most accepted classification of the Bivalvia was proposed by Bieler et al. (2010), in which Protobranchia is considered as a subclass, including the extant orders Nuculida Dall, 1889, Solemyida Dall, 1889 and Nuculanida Carter, Campbell and Campbell, 2000.

The monophyly of protobranchs has been established in some molecular analyses (Kocot et al., 2011; Smith et al., 2011; Sharma et al., 2012, 2013). However, others did not find uniform support for this monophyly (Bieler et al., 2014; Combosch et al., 2017; Lemer et al., 2019; Sato et al., 2020). Lemer et al. (2019) found that Solemyoidea is a sister group to all other bivalves, rendering Protobranchia paraphyletic. Non-monophyly of Solemyida (Solemyoidea + Manzanelloidea) was also obtained by Combosch et al. (2017).

The data of Sharma et al. (2013) unanimously supported four major clades of Protobranchia, which correspond to the superfamilies Nuculoidea Gray, 1824 (excluding Sareptidae), Nuculanoidea H. Adams and A. Adams, 1858 (including Sareptidae), Solemyoidea Gray, 1840 and Manzanelloidea Chronic, 1952. Salient aspects of the latter phylogeny include (1) support for the placement of the family Sareptidae with Nuculanoidea; (2) the non-monophyly of the order Solemyida; (3) and the non-monophyly of most nuculoid and nuculanoid genera and families.

The nuclear and combined gene datasets used by Sato et al. (2020) provided low support for the monophyly of Protobranchia; conversely, the monophyly of Nuculoidea, Solemyoidea, and Manzanelloidea was strongly supported. According to the latter authors, the most significant finding of their molecular analysis concerns the phylogenetic position of the family Sareptidae. This family includes the genera *Sarepta* and *Setigloma*, forming the superfamily Sareptoidea that is included in the order Nuculanida. The genus *Pristigloma* retains its own family Pristiglomidae in the superfamily Nuculanoidea (order Nuculanida).

These studies are reflected in the currently accepted classification of Protobranchia in the World Register of Marine Species (WoRMS, 2022) except for families Nucinellidae and Manzanellidae, maintained in the order Solemyoida.

Yonge (1939) studied the habits, structure, physiology of the organs in the mantle cavity and the nature of the gut in the three representative families of the protobranchs: Nuculidae, Solemyidae, and Nuculanidae. He concluded that the protobranchs represent one unquestionable natural group that is the more primitive among the bivalves. Since this review, scarce morphological studies on protobranchs have been carried out (Schaefer, 2000), most of which were related to particular species (Beedham and Owen, 1965; Morton, 2012; Simone, 2009; Stasek, 2009). Additional studies on physiology (Davenport, 1988) or embryogenesis (Zardus and Morse, 1998) have been also developed. An extensive review of the protobranch data was elaborated by Zardus (2002). All the above highlights the lack of specific studies on the ultrastructure of the mantle edge in this basal group.

Here, we study the morphology and function of the mantle edge together with the formation of the periostracum at ultrastructural level, in representatives of the three orders of Protobranchia, including one specimen of the type species in the family Sareptidae, in order to contribute to the knowledge of the morphology, functional biology and phylogeny of this subclass of Bivalves.

2. Material and methods

Ten species from three orders of Protobranchia were collected from southern Spain and Japan (Table 1, Fig. 1). The specimens were anesthetized for one hour with isotonic magnesium chloride solution (71 g of $MgCl_2.6H_2O$/liter of freshwater) prior to fixation. The number of specimens of each species used in the different histological procedures is indicated in Table 2.

Table 1
List of the studied species with data on sampling locality and habitat.

Species	Order	Family	Locality
Solemya elarraichensis P.G.Oliver, Rodriguez & Cunha, 2011	Solemyida	Solemyidae	Gulf of Cádiz, Spain (Anastasya mud volcano, 457 m) 36°31.35′N-7°9.07′W
Nucula nucleus (L., 1758)	Nuculida	Nuculidae	Málaga Bay, Spain (105 m, muddy bioclastic gravel) 36°36.49′N-4°21.75′W
Nucula hanleyi Winckworth, 1931	Nuculida	Nuculidae	Littoral of Mijas, Málaga, Spain (15–25 m, muddy bioclastic sand) 36°29′6 N-04°41.30′W
Nucula sulcata Bronn, 1831	Nuculida	Nuculidae	off Fuengirola, Málaga, Spain (64 m, muddy bottom) 36°32.13′N-4°33.44′W (methacrylate specimen) Málaga Bay (105 m, muddy bioclastic gravel) 36°36.49′N-4°21.75′W (TEM specimen)
Ennucula aegeensis (Forbes, 1844)	Nuculida	Nuculidae	Málaga Bay, Spain (105 m, muddy bioclastic gravel) 36°36.49′N-4°21.75′W
Acila insignis (Gould, 1861)	Nuculida	Nuculidae	off Sagami Bay, Japan (243–593 m) From 35°07.11'N-139°33.81′E to 35°06.95'N-139°33.47′E
Lembulus pella (L., 1758)	Nuculanida	Nuculanidae	Littoral of Granada, Spain (72 m, muddy sand) 36°41.56′N-3°20.76′W
Nuculana soyoae Habe, 1958	Nuculanida	Nuculanidae	off Misaki, Kanagawa Prefecture, Japan (96–98.7 m) From 35°07.82′N-139°34.34′E to 35°07.14′N-139°34.22′E
Saccella commutata (Philippi, 1844)	Nuculanida	Nuculanidae	Málaga Bay, Spain (105 m, muddy bioclastic gravel) 36°36.49′N-4°21.75′W
Sarepta speciosa A. Adams, 1860	Nuculanida	Sareptidae	Off Misaki, Kanagawa Prefecture, Japan (96.0–98.7 m) From 35°07.82′N-139°34.34′E to 35°07.14′N-139°34.22′E

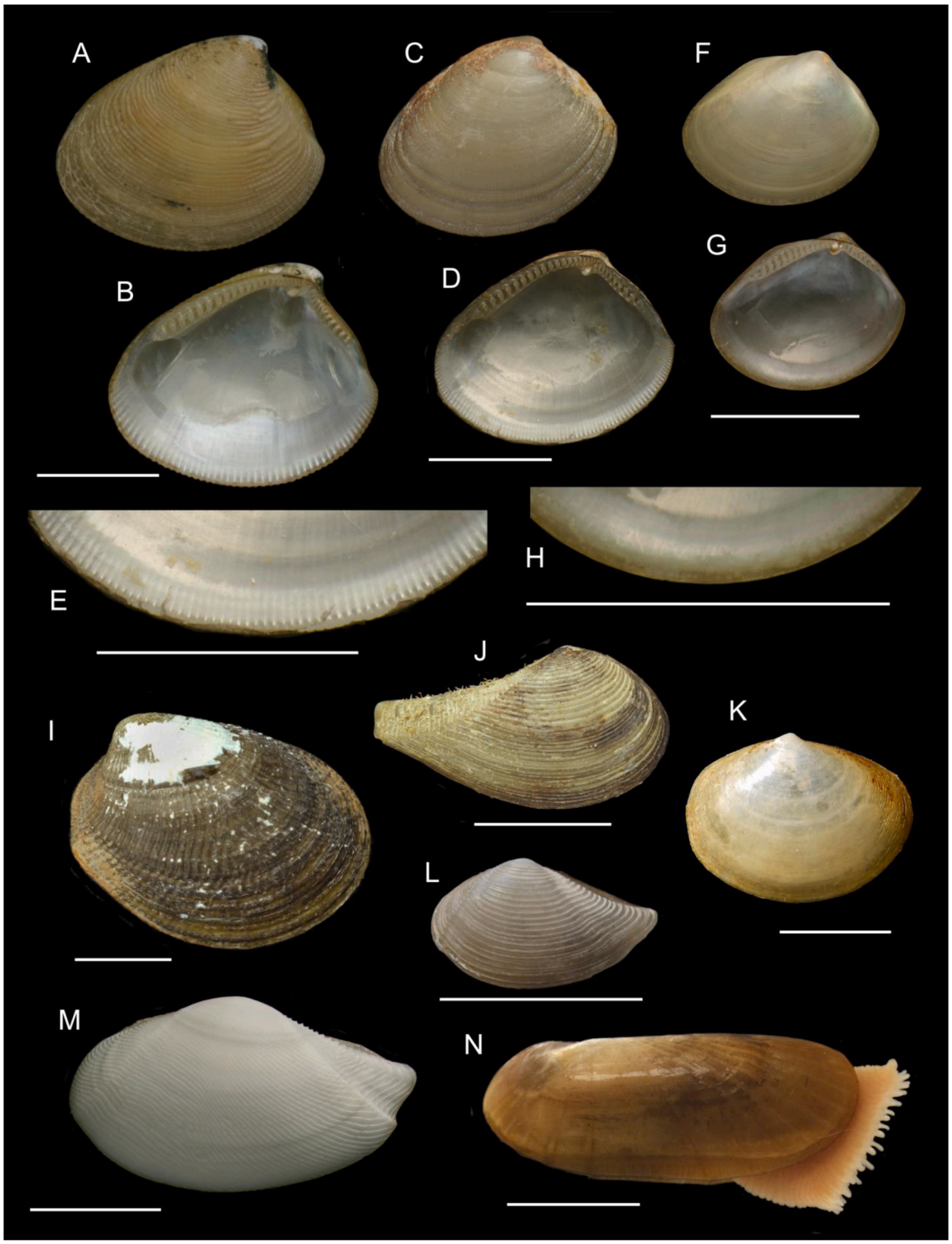

Fig. 1. Shells of the studied protobranch species. A, B. *Nucula sulcata* Bronn, 1831 from off Huelva, Spain (398 m). C-D. *Nucula nucleus* (L., 1758) from Medes Islands, Spain (10 m). E. Detail of the crenulated margin of *N. nucleus*. F-G. *Ennucula- aegeensis*(Forbes, 1844) from Alborán island platform, Alborán Sea (555 m). H. Detail of the smooth margin of *E. aegeensis*. I. *Acila insignis* (Gould, 1861) from Otsuchi Bay, Japan (University Museum, the University of Tokyo RM32230, 315 m). J. *Nuculana soyoae* Habe, 1958 from off Misaki, Japan (250 m). K. *Sarepta speciosa* A. Adams, 1860 from off Misaki, Japan (96.0–98.7 m). L. *Saccella commutata* from Chella Bank, Alborán Sea (210 m). M. *Lembulus pella* (Linnaeus, 1758) from off Mijas, Spain (15 m). N. *Solemya elarraichensis* Oliver, Rodriguez & Cunha, 2011 from Anastasya mud volcano, Gulf of Cádiz (457 m). Scale bar= 5 mm. Pictures of Japanese specimens courtesy of Kei Sato.

2.1. Light microscopy: paraffin and methacrylate embedding process

Specimens for histological procedures were fixed in 4% formaldehyde. Some of them were embedded in paraffin, sectioned at 7 and 10 μm, and stained with hematoxylin–eosin and hematoxylin-trichrome (Light Green, Orange G and Acid Fuchsine), according to Gutiérrez (1967). Paraffin sections were observed using an Olympus VF120 microscope.

Table 2
Number of specimens of each species used according to the histological procedure.

Species	TEM	SEM/FESEM	Methacrylate	Paraffin
S. elarraichensis	1			1
N. nucleus	2	1	2	
N. hanleyi	4	1		1
N. sulcata	2	1	1	
E. aegeensis	1			
A. insignis	1			
L. pella	2			1
N. soyoae	1			
S. commutata	3		1	3
S. speciosa	1			

In order to see the relationship between the mantle edge and the shell, one specimen of *Nucula nucleus* and *Nucula sulcata*, both of them with marginal crenulations, and one of *Saccella commutata*, without crenulations and with a very large inner mantle fold, fixed in formaldehyde (4%), were embedded in methacrylate at the Andalusian Center of Nanomedicine and Biotechnology (BIONAND), Málaga, Spain. The samples were dehydrated and embedded in Technovit 7200 VLC in five steps. The first three steps were mixtures of ethanol (ET) and Technovit (T) (30 T: 70ET; 50 T: 50ET; 70 T: 30ET) and the last two steps consisted only of Technovit 7200 VLC. The samples were subsequently polymerized. The embedded tissues were transversally sectioned to a thickness of 50 μm using the cutting band system EXAKT 300 CL. The sections were ground with a precision micro-grinding system EXAKT 400 C, stained with toluidine blue (1%, pH 8.3), and photographed with an Olympus VF120 microscope.

2.2. Transmission electron microscopy (TEM)

To study the ultrastructure of the mantle edge and the formation of periostracum, small pieces of the ventral free mantle edge were dissected and fixed in a mixture of 2.5% glutaraldehyde buffered with sodium cacodylate (0.1 M, pH 7.4) for at least 48 h at 4 °C and postfixed in OsO4 (2%) for 2 h at 4 °C, then embedded in epoxy resin Aname Epon 812 (EMS) and Spurr low viscosity embedding resin (EMS). A minute specimen of *Ennucula aegeensis* was entirely fixed in a mixture of 2.5% glutaraldehyde buffered with sodium cacodylate (0,1 M, pH7.4). After this, it was completely decalcified by immersion in 2% EDTA (Ethylene Diamine Tetraacetic Acid) and then embedded in Spurr resin.

Semithin sections (0.5–0.6 μm) were stained with toluidine blue (1%, pH 8.3) and were observed using an Olympus VF120 microscope. Ultrathin sections (0.1 μm) were stained with uranyl acetate (1%) followed by lead citrate and examined with a TEM ZEISS EM at the University of Granada, TEM FEI Talos 200X with EDX system at the University of Málaga and Thermofisher Scientific Tecnai G2 20 Twin, at the ICTS "NANBIOSIS" U28 unit of the IBIMA Plataform BIONAND.

2.3. Scanning electron microscopy (SEM) and field-emission scanning electron microscopy (FESEM)

To observe the second outer fold in relation with the crenulations of the mantle edge, a living specimen of the crenulated species *Nucula sulcata,* the largest species of *Nucula* studied, was selected for SEM view. For this purpose, it was fixed in 4% formaldehyde for a week, after which, the soft parts were dehydrated by increasing concentrations of ethanol (50%, 70%, 90% and 100%) at room temperature, each step for 20 min. They were then critical point CO_2 dried and sputter-coated with gold. Finally, they were visualized in a SEM JEOL-JSM840 at the University of Málaga.

To better understand the relationship between the second outer fold, crenulations and shell crystallography, valves of *N. hanleyi* and *N. nucleus* were coated with carbon (Hitachi UHS evaporator) for observation of the marginal crenulations in a field-emission scanning electron microscope (FESEM) Zeiss Auriga Cross-Beam Station from the Centro de Instrumentación Científica (CIC) of the University of Granada (UGR).

3. Results

3.1. Mantle edge

The mantle edge of the studied protobranchs showed morphological differences between families and even between genera of the same family. Some of these differences are related to the number of folds and others to their morphology. Regarding the number of mantle folds, although the general rule among bivalves is the presence of three mantle folds: an outer fold (hereafter OF), a middle fold (hereafter MF) and an inner fold (hereafter IF), the crenulated species of the genus *Nucula* (*N. hanleyi*, *N. nucleus* and *N. sulcata*) showed a second outer fold at the outer surface (shell side) of the OF (Figs. 1A-E; 2A-D), in contrast to the non-crenulated species (*Acila insignis* and *Ennucula aegeensis*) (Figs. 1F-H; 2E,F), the nuculanids (Fig. 2G-L) and *Solemya* (Fig. 3A-B). *Sarepta speciosa* (Fig. 2K-L), the type species of the genus *Sarepta,* did not exhibit this second outer fold; but it did present minute OF and MF and a very long and ciliated IF, in which blood sinuses were frequent.

The second outer fold of crenulate nuculids was either slightly projected onto the internal layer of the shell or appressed against the OF outer epithelium, then becoming inconspicuous (Figs. 2A,B; 3C-G). In large specimens of *N. sulcata* the second outer fold can occur very far from the distal margin of the OF (Fig. 3F-H), making it possible to see by low magnification SEM (Fig. 4A) but which may hinder its observation in semithin and TEM sections. The inner mantle fold was large and it was found in a quite distal position with respect to the periostracal groove (Fig. 3H).

The basal cells of the minute non-crenulated *Ennucula aegeensis* that secrete the periostracal pellicle were projecting between the middle and outer folds, and thereby acquiring the appearance of a small intercalated fold (Fig. 4B). As a consequence, the inner OF epithelium reaches the bottom of the periostracal groove and then folds outwards, dragged by the basal cells (Fig. 4C).

The OF and MF in the nuculanids *Saccella commutata* and *Lembulus pella* were simple and relatively small, while the IF was long and flexible in *S. commutata* (Fig. 2G-I). In *L. pella* and *N. soyoae* the IF was no longer than the MF but is very folded (Fig. 2I,J). The MF was frequently split, with the small outer sub-fold functioning as a guide for orienting the periostracum toward the outer side of the OF (Fig. 2A,B,C,E,I).

Solemya elarraichensis, the only studied species of the order Solemyida, exhibited a broad, flexible three folded mantle edge (Fig. 3A), which was directed toward the pallial cavity along the large anterior pedal aperture. The mantle edges were fused from the posterior inhalant aperture to the beginning of the pedal aperture at the middle of the ventral side. The OF inner epithelium was prolonged very far from the periostracal groove (Fig. 3A), the MF was short but relatively thick (Fig. 3B) and the IF was very long, wide and very flexible (Fig. 3A). At the beginning of the IF, beneath the periostracal groove, an oil duct section (as defined by Beedham and Owen, 1965 among others) was visible (Fig. 3B, arrow). The OF inner epithelium appeared to be involved in the secretion of a fine layer of periostracum that acquired a green color with the trichromic staining and that maintained the same thickness along the periostracum (Fig. 3A). The shell side mantle epithelium seems to be also involved in the thickening of the periostracum, forming a layer that acquired a red color with the thickening process, after the trichromic stain (Fig. 3A).

Other salient features of the mantle edge among the studied protobranchs was that the mantle folds were frequently folded (Fig. 2E,H,J). In some cases, like in *N. sulcata,* the flexibility of the IF helped to take up particles (Fig. 3H). Folding of the OF epithelium both in the periostracal groove (e.g. *A. insignis*) and on the outer (shell side) surface (e.g.

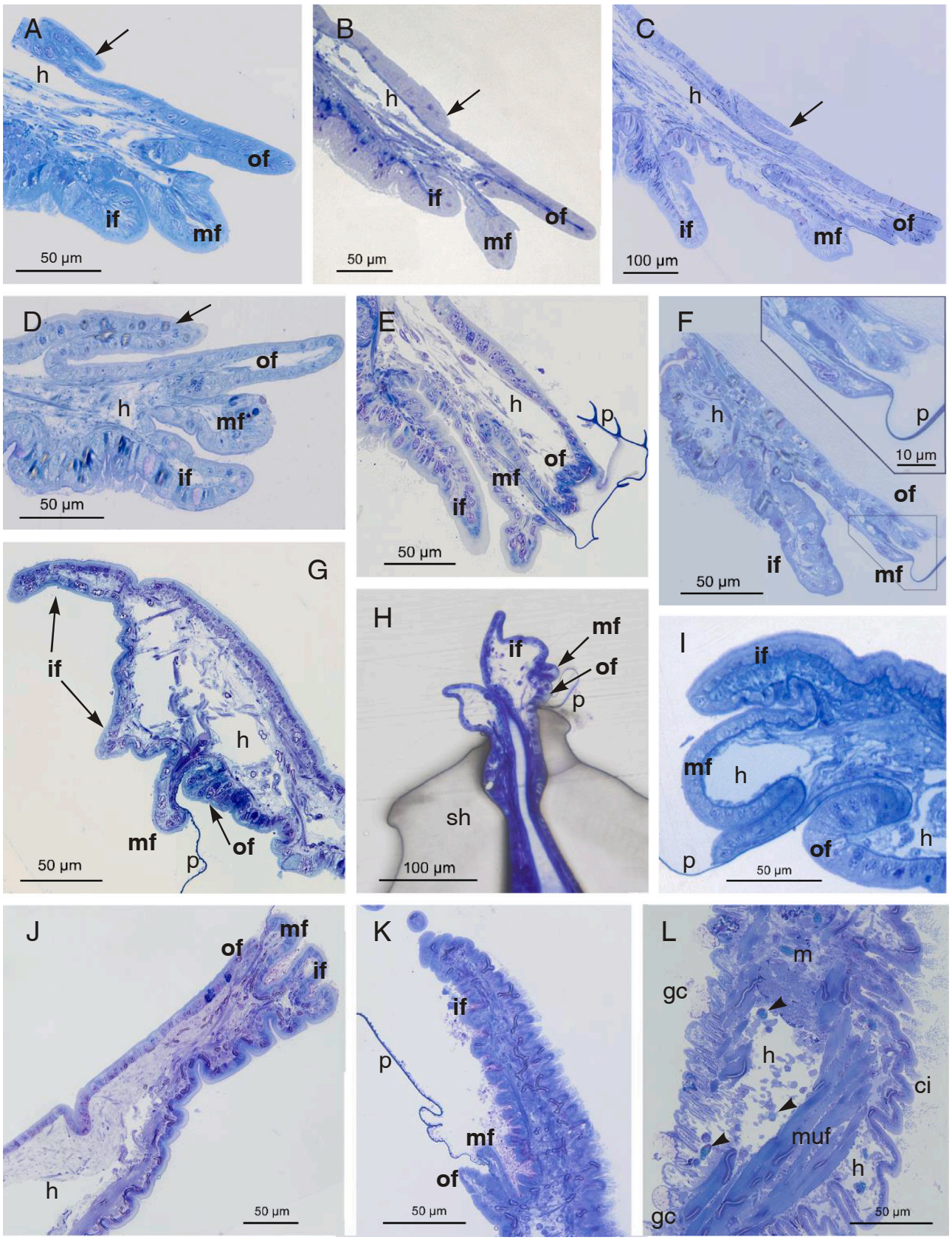

Fig. 2. Methacrylate (H) and semithin (all others) sections of protobranchs showing the mantle folds. A. *Nucula hanleyi* with the second outer fold (arrow) visible. B. *N. hanleyi* with the second outer fold appressed against the outer fold epithelium. C. *N. sulcata* showing the second outer fold (arrow). D. *Nucula nucleus* showing the second outer fold (arrow). E. *Acila insignis* without second outer fold and with folded periostracum. F. *Ennucula aegeensis* with minute fold inside the periostracal groove. G-H. *Saccella commutata*. I. *Lembulus pella*. J. *Nuculana soyoae*. K. *Sarepta speciosa.* L. Mantle section of *Sarepta speciosa* with arrowhead showing granulocytes. ci: cilia; gc: glandular cell; h: blood sinus; if: inner fold; m: mantle; mf: middle fold; muf: muscular fibers; of: outer fold; p: periostracum; sh: shell.

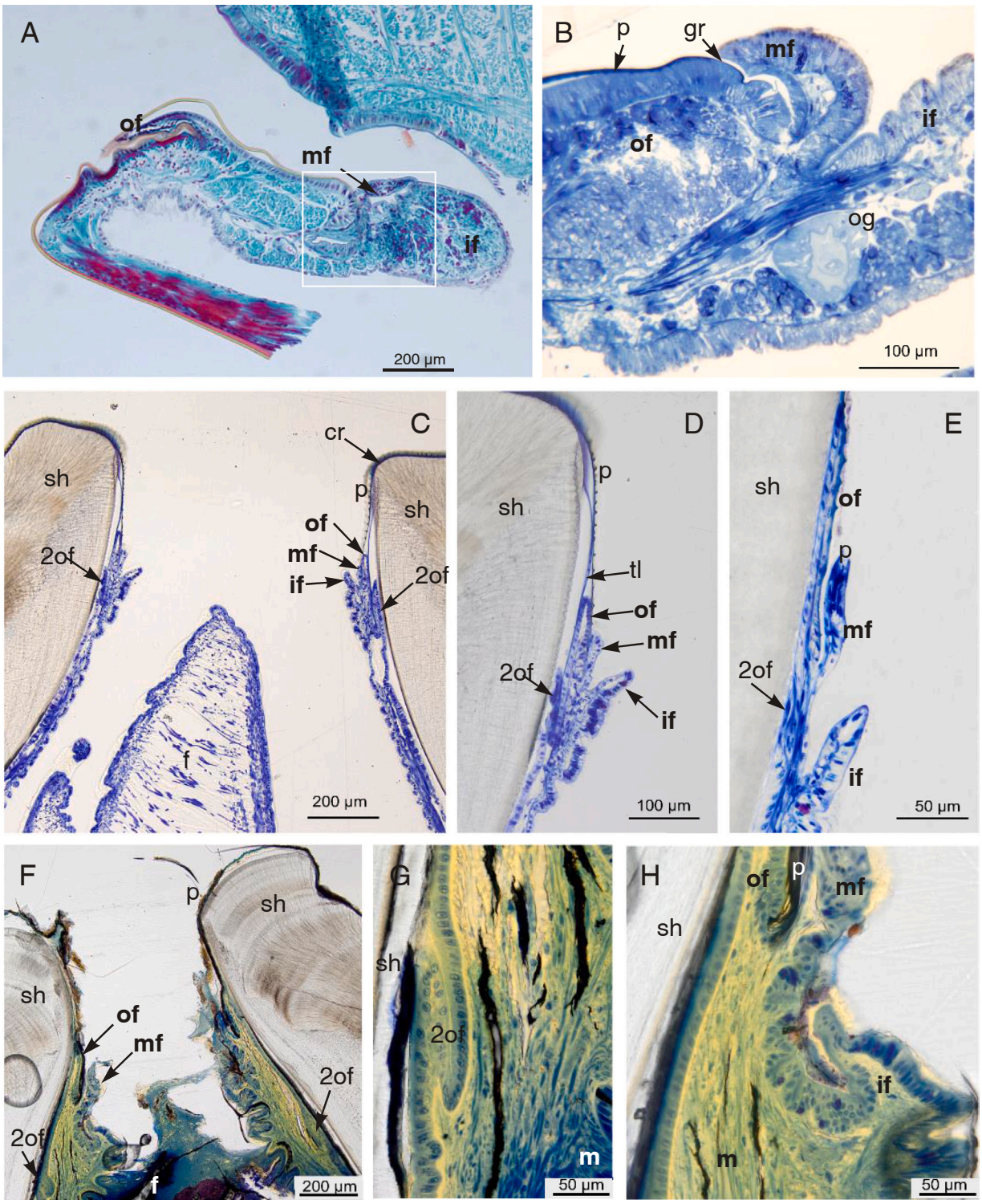

Fig. 3. Paraffin (A), semithin (B) and methacrylate (C-H) sections of the mantle edge in some protobranchs. A. *Solemya elarraichensis,* mantle folds and part of the mantle. B. Periostracal groove (frame in A) with section of an oil gland (og) under the periostracal groove. Methacrylate sections of *Nucula nucleus* (C-E) and *Nucula sulcata* (F-H). C,F. Views of part of the foot and mantle folds. D. Detail of the left mantle folds showing the second outer fold functioning as template for crenulation. E. Detail of the left mantle showing the second outer fold appressed against the outer fold in the crenulation zone. G. The second outer fold appressed against and in continuity with the mantle epithelium. H. The inner fold helping to take up food particles. f: foot; gr: periostracal groove; if: inner fold; m: mantle; mf: middle fold; of: outer fold; og: oil gland; p: periostracum; sh: shell; 2of: second outer fold.

E. aegeensis) was frequent (Fig. 5A,B). In the latter species, voluminous glandular cells appeared along the shell side mantle epithelium (Fig. 5C, D). The secretions were discharged, like many vesicles, to the extrapallial space (Fig. 5E,F), which was delimited, after the decalcification process, by a dense organic network. The mantle folds seemed very elastic, helping to maintain epithelial cell connections. There were also strong interdigitations of the cellular membranes between adjacent cells in all the species of nuculids and nuculanids (Fig. 5G-L). Along the interdigitated intercellular membranes, conspicuous adherens junctions near the apical surface were visible (Fig. 5H,J,K).

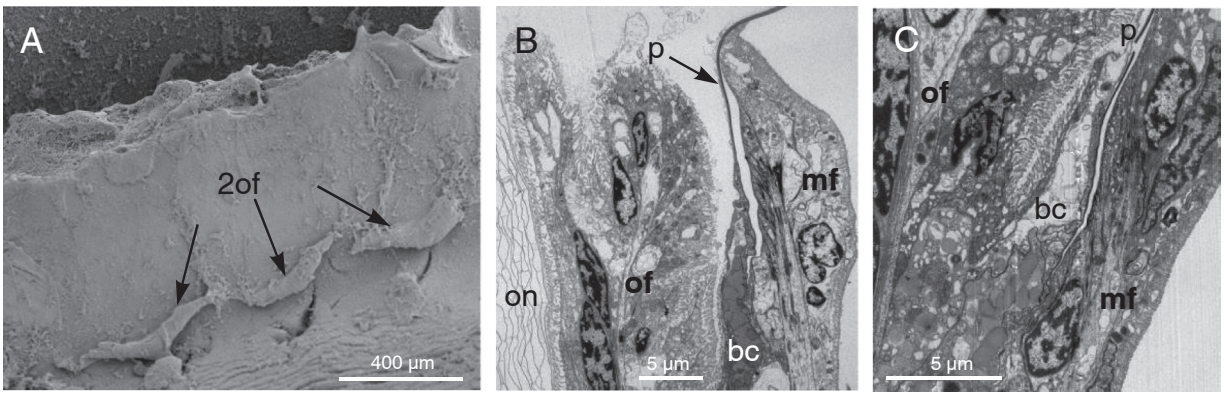

Fig. 4. A. SEM view of the second outer folds (black arrows) at the base of the crenulations in *Nucula sulcata*. B. TEM view of the mantle edge of *Ennucula aegeensis* showing the protrusion of the glandular basal cells into the periostracal groove between the outer and middle folds. The periostracum runs out between the glandular basal cells and the middle fold. C. View of the inner epithelium of the outer fold folded at the bottom of the periostracal groove to be dragged by the basal cells. bc: basal cells; if: inner fold; mf: middle fold; of: outer fold; on: organic network of the shell; p: periostracum; 2of: second outer fold.

Some scattered sensorial cells were present, mainly between the epithelial cells of the MF, but also in the IF, more abundant in the ciliate epithelium. These cells were frequently narrow, with a dense cytoplasm and finger-like projections or cilia, although other types with a depressed microvillous border can be present (Fig. 6A,B). The latter are recognizable as sensorial cells due to the presence of nerve fibers and glial cells near the basal membranes. The glial cells present electron-dense granules in their cytoplasms (Fig. 6B). *Solemya elarraichensis*, a very deep burrowing species, presented bacteriocytes in the inner epithelium of the middle fold (Fig. 6C); but no sensory cells were observed.

Intense but differentiated secretion was present in all the epithelial cells of the mantle folds. Continuous formation of vesicles appeared in the inner epithelium of the OF, inside the periostracal groove (Fig. 7A). The OF inner layer is responsible for the thickening of the periostracum, but in the crenulated species of *Nucula* a conspicuous dense periostracal layer was also secreted by the OF epithelium outside the periostracal groove (Fig. 7B), connecting with the free periostracum at the internal margin of the valves (Fig. 3C-E). Many vesicles secreted by the OF inner epithelium showed an electron-dense content of protein-like vesicles (Fig. 7C). Formation of vesicles was also observed within the furrow between the OF and the fourth fold (Fig. 7D) but was particularly intense at the shell side epithelium of the second outer fold in crenulated *Nucula* spp (Fig. 7E-F).

The MF outer surface (periostracal groove side) also showed active secretion that does not seem to be involved in the growth of the periostracum because the pellicle does not increase in thickness (Fig. 7G-H). The inner MF epithelium also showed secretion of glycocalix, such as that observed in *S. elarrachensis* (Fig. 7I).

Intense secretion of glycocalix was present in the whole IF epithelium of all examined protobranchs (Fig. 8A-C), mainly in nuculanids. A ciliated area was present in the IF pallial epithelium and continued along the inner mantle surface in the nuculids and nuculanids (Figs. 2A-G, I-L; 3C-D,H). The function of these cilia seem also to be related to the capture of particles and microorganisms (Fig. 8D-E), although the microvilli, together with secretion of glycocalix, were also able to capture particles introduced in the cells by numerous endocytic vesicles, most of them transported through the intercellular membranes (Fig. 8F-G). Numerous lysosomes were also present under the microvilli (Fig. 8H) together with high amount of glycogen-like granules in the cytoplasm of many IF epithelial cells (Fig. 8I). All the latter point to active metabolism by the epithelial cells of the IF.

3.2. Periostracum: formation and structure

3.2.1. Basal cells

The periostracum in all the analysed species originated at the bottom of the periostracal groove, by secretions from two basal cell rows that belong to the OF (Fig. 9A-D). These cells lack microvilli and have folded free apical membranes (Fig. 9E). In nuculids and some nuculanids one row of these basal cells had a high density of secretory vesicles; some of them resembling lipid-protein vesicles, hence their designation as glandular basal cells (Fig. 9B,F). There was, as a general pattern, a conspicuous vacuolar space adjacent to the basal cells where the secretory vesicles seemed to accumulate their secretions (Fig. 9B,C,F). In general, the periostracum ran along and across the periostracal groove close to the MF (Fig. 2E-G,I-K).

The basal cells in Nuculidae were located towards the middle of the OF inner surface, because the MF outer epithelium crossed the bottom of the periostracal groove and invaded the proximal inner side of the OF (Fig. 9A). A particular case is the minute non-crenulated *E. aegeensis*, in which the elongate glandular basal cells projected inside the periostracal groove, and the periostracum ran between this small "fold" and the MF, at first close to the basal cells, but later close to the MF (Fig. 4B,C). In Nuculanidae, the MF epithelium hardly surpassed the bottom of the periostracal groove (Fig. 9B). *Solemya speciosa* showed a pattern similar to that found in other nuculanids (Fig. 9C). This species had both basal cells just at the bottom of the periostracal groove, between the OF and MF epithelia, without the presence of vacuolar space for the basal cell secretions; nevertheless, the periostracum was slightly curved at the beginning (Fig. 9D).

3.2.2. Structure of the periostracum

A layered pattern is the general rule of the periostracum of Protobranchia. Three layers were present in the studied species: (1) a nanometric external membrane, termed pellicle (p), ill-defined in some groups such as Solemyidae; (2) a second well defined dark layer (DL) and (3) a translucent layer (TL) that eventually becames tanned to form the dark layer (Fig. 9G-J).

The "pellicle" is a thin membrane, initially secreted as a network of small filaments (about 10–12 nm) in the space between the basal cells and the first cell of the MF (Fig. 9A,E), where a vacuolar space, more or less conspicuous, can be present and where the secretion of the basal cells would be eventually accumulated (Fig. 9B,F). Afterward, the network fused to form the pellicle, about 100 nm thick. The thickness of the pellicle was constant along the periostracum, indicating that its secretion only depends on the basal cells. The pellicle was well defined in nuculanids (Fig. 9G-H), particularly in *L. pella* (Fig. 9G) and some nuculids (Fig. 9I) but ill-defined in other nuculids, such as *N. sulcata*

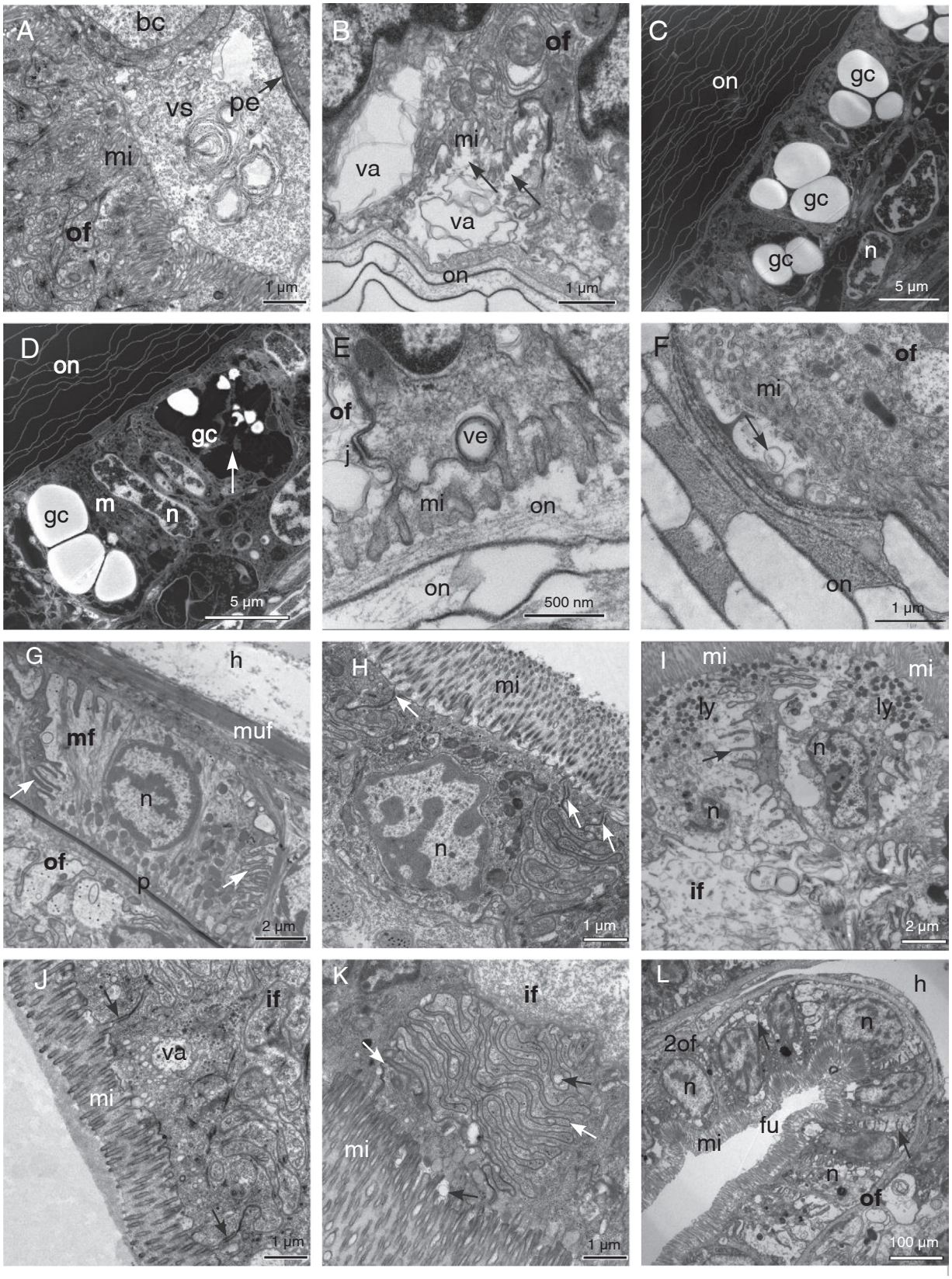

(caption on next page)

Fig. 5. TEM views of the folding and secretions of the mantle folds in nuculids (A-F) and the strong interdigitation (black and white arrows) between adjacent epithelial cells of the mantle folds (G-L). A. Inner epithelium of the outer fold at the bottom of the periostracal groove in *Acila insignis*. B. Folding (black arrows) of the outer epithelium of the outer fold in *Ennucula aegeensis*. C-D. TEM STEM views of the glandular cells from the mantle epithelium in *Ennucula aegeensis*; one of them (D) is partially discharged (white arrow). E. Secretion of vesicles by the outer epithelium of the outer fold in *Ennucula aegeensis*, together with part of the organic shell network. F. Secretion of vesicles by the outer epithelium of the outer fold in *Nucula hanleyi* with part of the organic network (black arrow) of the shell. G. Middle fold of *Nucula sulcata* from the periostracal groove. H. Inner fold of *Sarepta speciosa*. I. Inner fold of *Saccella commutata.* Black arrow shows the vacuoles that transport material through the interdigitating intercellular space. J. Inner fold of *Acila insignis* with presence of numerous vacuoles and adherens junctions (black arrows). K. Inner fold of *Nuculana soyoae*, with transport of vacuoles (black arrows) through the interdigitating intercellular space (white arrows). L. Furrow between the outer fold (left epithelium) and the second outer fold (rigth epithelium) of *Nucula nucleus*. bc: basal cells; fu: furrow between the outer fold and the second outer fold; gc: glandular cell; h: blood sinus; if: inner fold; ly: lysosome; m: mantle; mf: middle fold; mi: microvilli; muf: muscular fibers; n: nucleus; of: outer fold; on: organic network of the shell; p: periostracum; va: vacuole; ve: vesicle; vs: vacuolar space; 2of: second outer fold.

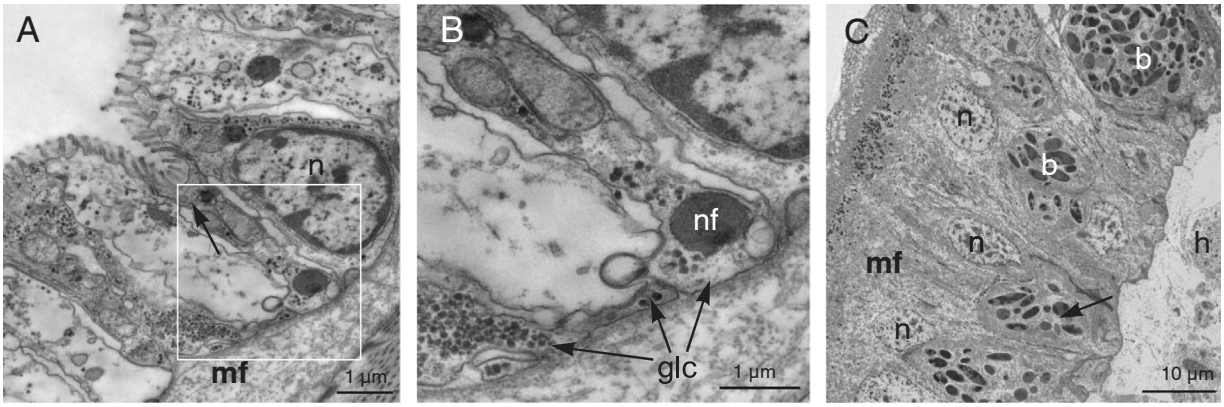

Fig. 6. A. TEM views of a sensorial cell (black arrow) in the middle mantle fold of *Saccella commutata* B. Detail of the frame in A to show a nervous fiber section and glial cells. C. TEM view of the bacteria in the bacteriocytes (black arrow) in the inner epithelium of the middle mantle fold of *Solemya elarraichensis*. b: bacteria; glc: glial cells; h: blood sinus; mf: middle fold; n: nucleus; nf: nervous fiber.

(Fig. 9J), or in *S. elarraichensis* (Fig. 10A-B).

The dark layer (DL) is formed by sclerotization of the OF translucent secretion (TL) that can be more or less quickly tanned. In all the studied protobranchs the thickening of the periostracum continued outside the periostracal groove, secreted by the epithelial cells of the ventral (distal) edge and by part of the outer OF epithelium. In the case of the crenulated species of *Nucula* (*N. sulcata, N. nucleus, N. hanleyi*) the secretion of a translucent layer also occurred along the outer OF epithelium up to the beginning of the second outer fold (Fig. 9B). This translucent secretion from the outer OF joined the periostracum before it reaches the edge of the valves (Fig. 3C-E).

The presence of isolated vesicles of translucent secretion inside the dark layer at the base of the periostracal folds was frequent in nuculanids and in *Solemya*. *Solemya elarraichensis* exhibited one small pouch of TL inside the DL underneath each periostracal micro-projection (Fig. 10A), eventually embedded in a continuous and very wide DL as the periostracum emerged from the periostracal groove (Fig. 10B). The secretion of the periostracum in this species extended considerably along the inner and outer OF epithelium, outside the periostracal groove (Fig. 3A). The thickening of the periostracum continued along an extended surface of the mantle epithelium showing a marked extension beyond the calcareous portion of the valves. The trichromic stain (VOF) produced intense red color in the mantle cells and in the inner layer of the periostracum (Fig. 3A). The latter could be related to the presence of elastic fibers. Due to the extensive epithelium involved in its secretion and thickening, the periostracum of *S. elarraichensis* is very thick, reaching more than 2 µm at the end of the periostracal groove.

Among the nuculanids, *L. pella* showed continuous translucent and dark layers from the bottom of the periostracal groove to the free periostracum (Fig. 9G). *Saccella commutata* presented small vesicles of translucent layer inside the dark layer beneath each periostracal fold. This pattern appeared inside the periostracal groove (Fig. 10C), while outside the periostracal groove, the dark layer was continuous without translucent pouches (Fig. 10D). Conversely, in *N. soyoae* a thick rim of dark layer was formed at the bottom of the periostracal groove under each periostracal fold (Fig. 10E), but in the free periostracum the dark layer became continuous (Fig. 10F) as in *Saccella*. Among the nuculids, *Acila insignis* presented a vesicular structure along the incipient periostracum inside the periostracal groove (Fig. 10G) but in the free periostracum the vesicles became concentrated as pouches of translucent layer inside and under the dark layer folds at the periostracal folds (Fig. 10H). *Nucula hanleyi* and *E. aegeensis* showed a continuous vesicular layer that was sealed by two dark layers (Fig. 11A-H). *Nucula hanleyi* had a vesicular structure along the whole periostracum, underneath the pellicle. These vesicles were pouches of translucent secretion coated by sclerotized secretion (DL) that were originated by the secretion of nanometric vesicles (ca. 100–200 nm) from the microvilli of the inner epithelium of the OF (Fig. 11A-B). Only the translucent secretion outside the vesicles will become tanned along the periostracal groove. These vesicles begin at the bottom of the periostracal groove (Fig. 11A). At the gaping end of the periostracal groove, the vesicles acquired an elongate morphology, underneath a continuous DL and above a continuous TL (Fig. 11C). The latter TL underneath the vesicles will eventually become sclerotized to form a dark layer connecting with the forming shell (Fig. 11D). *Ennucula aegeensis* showed a three-layered non-vesicular periostracum formed inside the periostracal groove (Figs. 9I, 11E), while outside the groove, the free periostracum formed a vesicular layer similar to that of *N. hanleyi*, with a continuous dark layer underneath the vesicles (Fig. 11F-H). In *N. sulcata* (Fig. 9J) and *N. nucleus* there was no vesicular structure in the periostracum, which showed a continuous dark layer both inside and outside the periostracal groove.

The translucent layer of *Sarepta speciosa*, when inside the periostracal groove, formed isolated pouches enclosed within each fold of the dark layer (Figs. 7G, 11I), but at the end of the periostracal groove, the periostracum stretched out and these pouches of translucent layer coated by dark layer spread out beyond the folds to become a continuous vesicular layer (Fig. 11J-L) that will also be sealed by a dark layer to connect with the shell.

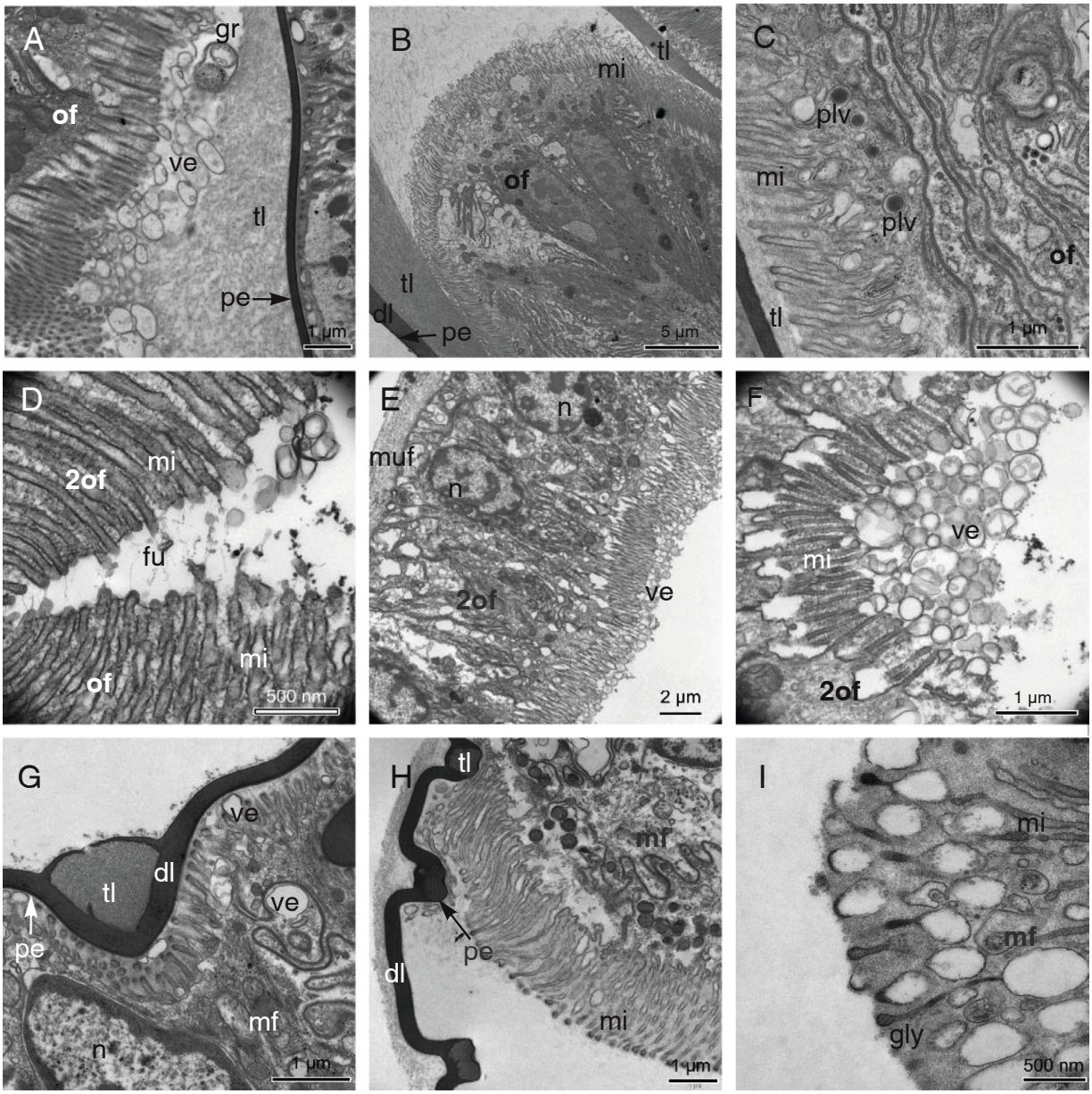

Fig. 7. TEM views of the secretions of the epithelial cells of the outer mantle fold (A-C), outer and second outer folds (D), second outer fold (E-F) and middle mantle fold (G-I). A. Vesicular secretion into the periostracal groove in *Nucula sulcata* to form translucent layer. B. Secretion of dense translucent layer of the periostracum inside and outside the periostracal groove in *Nucula sulcata*. C. Secretion of protein-like vesicles with electron-dense content into the periostracal groove in *Acila insignis*. D. Secretion in the furrow formed between the outer and the second outer folds in *Nucula nucleus*. E. Intense vesicular secretion by the outer (shell side) epithelium of the second outer fold in *Nucula nucleus*. F. Detail of the vesicles from E. G. Secretion of middle mantle epithelium into the periostracal groove in *Sarepta speciosa.* H. Secretion of middle mantle epithelium at the end of the periostracal groove in *Saccella commutata*. I. Glycocalix secretion by the microvilli of the inner epithelium of the MF in *Solemya elarraichensis*. dl: dark layer; fu: furrow between the outer fold and the fourth fold; gly: glycocalix; gr: periostracal groove; mf: middle fold; mi: microvilli; n: nucleus; of: outer fold; p: periostracum; pe: pellicle of the periostracum; plv: protein-like-vesicles; tl: translucent secretion by the outer fold; ve: vesicle; 2of: second outer fold.

A summary of the main results is present in Table 3.

4. Discussion

4.1. Mantle edge: form and function

The mantle edge in Bivalves presents, as a general rule, three lobes (or folds), outer, middle and inner (Yonge, 1939, 1957), although two folds have been described in some Arcidae (Waller, 1978), four folds in Veneridae (Ansell, 1961; Hillman and Shuster, 1966) and up to five in the venerids *Megapitaria aurantiaca* and *M. squalida* (García-Gasca and García-Domínguez, 1995). A high morphological variability of these folds has also been described in bivalves (Audino and Marian, 2016, 2018). There is only consensus on the homology of the periostracal gland (basal cell) and periostracum, and of the outer shell-secreting fold (OF) (Waller, 1978).

Different embryological origins for the middle fold have been assumed: (a) by a longitudinal splitting of the outer fold during the development (Quayle, 1952 for *Venerupis pullastra*) or (b) by folding of the inner fold (Audino et al., 2015 for *Nodipecten nodosus*). Morton and Peharda (2008) considered that the bivalve mantle edge has evolved from a bi-folded to a three-folded structure both ontogenetically and phylogenetically. The presence of three or more folds in the basal clade of Protobranchia seems to refute the bi-folded mantle edge as

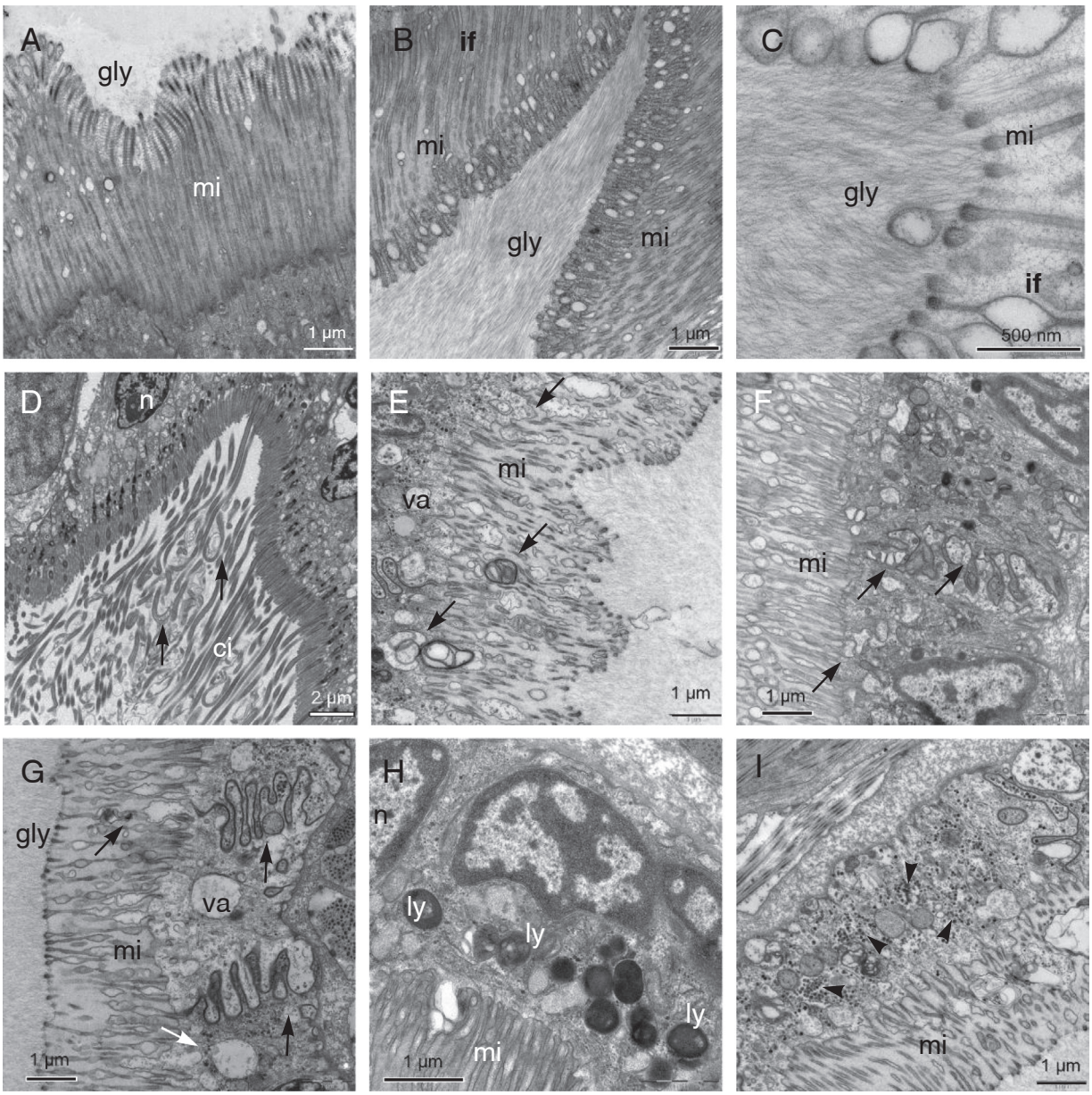

Fig. 8. TEM views of the secretion of glycocalix and uptake of particles by the inner epithelium (A-F) and transport of the particles by vacuoles through the interdigitating intercellular zones (G-I). A. Glycocalix secretion by the microvillous epithelium of the inner mantle fold in *Sarepta speciosa*. B. Intense secretion of glycocalix inside a furrow of the inner mantle fold in *Nuculana soyoae*. C. Secretion of glycocalix by the microvilli of the inner mantle fold in *Lembulus pella*. D-E Capture of particles (black arrows) by cilia from the inner mantle fold in *Ennucula aegeensis* (D) and *Saccella commutata* (E). F. Numerous endocytic vesicles (black arrows) are present at the distal cytoplasm of *Lembulus pella*. G. Large vacuoles (white arrow) and transport through the intercellular membranes (black arrows) in *Saccella commutata*. H. Presence of numerous lysosomes under the microvilli in *Nuculana soyoae*. I. Presence of numerous glycogen-like granules (black arrowheads) in the cytoplasm of *Saccella commutata*. ci: cilia; gly: glycocalix; if: inner fold; ly: lysosomes; mi: microvilli; n: nucleus; va: vacuole.

plesiomorphic state in the evolution of bivalves.

Nucula nucleus, N. hanleyi, and *N. sulcata* have crenulations on the internal margin of the valves, contrary to the other studied nuculids (*Acila insignis, Ennucula aegeensis*), nuculanids (including *Sarepta speciosa*) and *Solemya elarraichensis*. The small second lobe located at the outer OF, when is slightly projected toward the shell, along with the dense TL secreted by the outer OF epithelium, seems to function as template for the formation of the valve marginal crenulations. This is similar to the setting found in Cardiidae, in which projections in the outer side of the OF function as "templates" for the formation of the radial ribs (Stone, 1998; Checa and Jiménez-Jiménez, 2003). Stone (1998) called these OF projections "corpora spinosa".

The intense secretion of the translucent layer of the periostracum around the OF observed in these crenulated nuculids could be related to the process of calcification of the crenulations, which are even visible with closed valves. Due to the attitude of this small second outer fold, raised or flattened, it has not been recognized in previous observations when appressed against the OF outer epithelium, in line with the mantle; therefore Checa and Salas (2017) concluded that the Protobranchia have three mantle fold as a general rule. The absence of this second outer fold in *Acila insignis*, without crenulations on the shell margin, would indicate that it is not a phylogenetic character but a morphological adaptation for the formation of the crenulations. A special case is the minute *Ennucula aegeensis*, without marginal crenulations and without a second outer fold. The smooth margin of the juveniles of crenulated *Nucula nucleus*, *N. hanleyi* and *N. nitidosa* raises the hypothesis on a

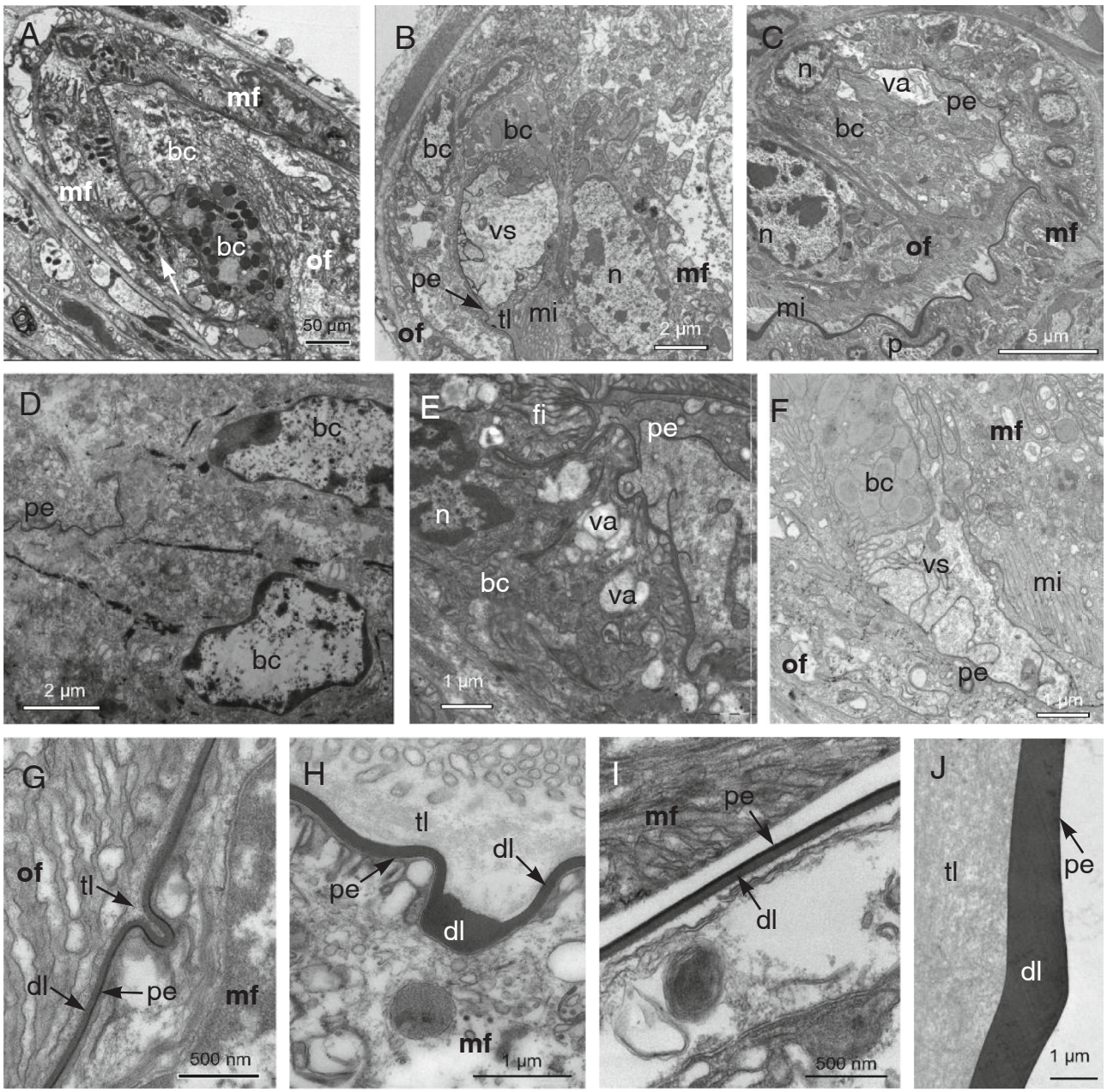

Fig. 9. TEM views of the basal cells (A-F) and the structure of the periostracum (G-J). A. Glandular basal cell of *Nucula nucleus,* with nanometric filaments (white arrow) at the beginning of the periostracum. B. Very developed glandular basal cell and large vacuole at the beginning of the periostracum in *Lembulus pella.* C. Basal cells and vacuole in *Sarepta speciosa.* D. Both basal cells in *Solemya elarraichensis.* E. Very infolded basal cell of *Nuculana soyoae* with view of the nanometric filament of the incipient pellicle. F. View of the initial pellicle with the nanometric filaments in the vacuolar space in *L. pella*. G. Layered periostracum inside the periostracal groove in *Lembulus pella*, with very defined pellicle. H. Defined pellicle and dense dark layer of the periostracum inside the periostracal groove in *Saccella commutata*. I. Periostracum at the bottom of the periostracal groove in *Ennucula aegeensis*. J. Periostracum at the distal periostracal groove with ill-defined pellicle, well defined dark layer and very thick translucent layer in *Nucula sulcata*. bc: basal cell; dl: dark layer; fi: nanometric filaments; mf: middle fold; mi: microvilli; n: nucleus; of: outer fold; p: periostracum; pe: pellicle of the periostracum; tl: translucent secretion by the outer fold; va: vacuole; vs: vacuolar space.

paedomorphic origin of this species (Gofas and Salas, 1996). The latter seems to be corroborated by the vesicular structure of the free periostracum in *E. aegeensis* that is similar to that found in *Nucula hanleyi*. The crenulations in epibenthic *Nucula* spp may be an adaptive trait directed to maintain a strong valve closure for preventing predator attacks, which are likely more intense on the continental shelf. The minute glandular fold, between the OF and MF of *E. aegeensis,* could be a different adaptive feature, related to miniaturization and needed for maintaining the functional extension of the OF secretory epithelium.

There is a general consensus regarding the functions realized by the mantle folds: secretion of the periostracum and calcareous layer by the outer fold, sensory detection by the middle fold and muscular activity by the inner fold (Yonge, 1939). In the crenulated nuculids, the whole OF epithelium secretes translucent layer (TL) contrary to other bivalves, where the OF outer surface does not secrete periostracum (Checa and Salas, 2017). However, the formation of the shell ostracum (aragonitic prisms) in crenulated nuculids seems to be also carried out by the OF while the second outer fold would secrete nacre (Fig. 12A-B, D-E) and for which intense vesicle secretion has been observed (Fig. 7E-F). Taking into account all the latter, the second outer fold would be considered a projection of the mantle that would function as template for the formation of the crenulations like the "corpora spinosa" in Cardiidae for the

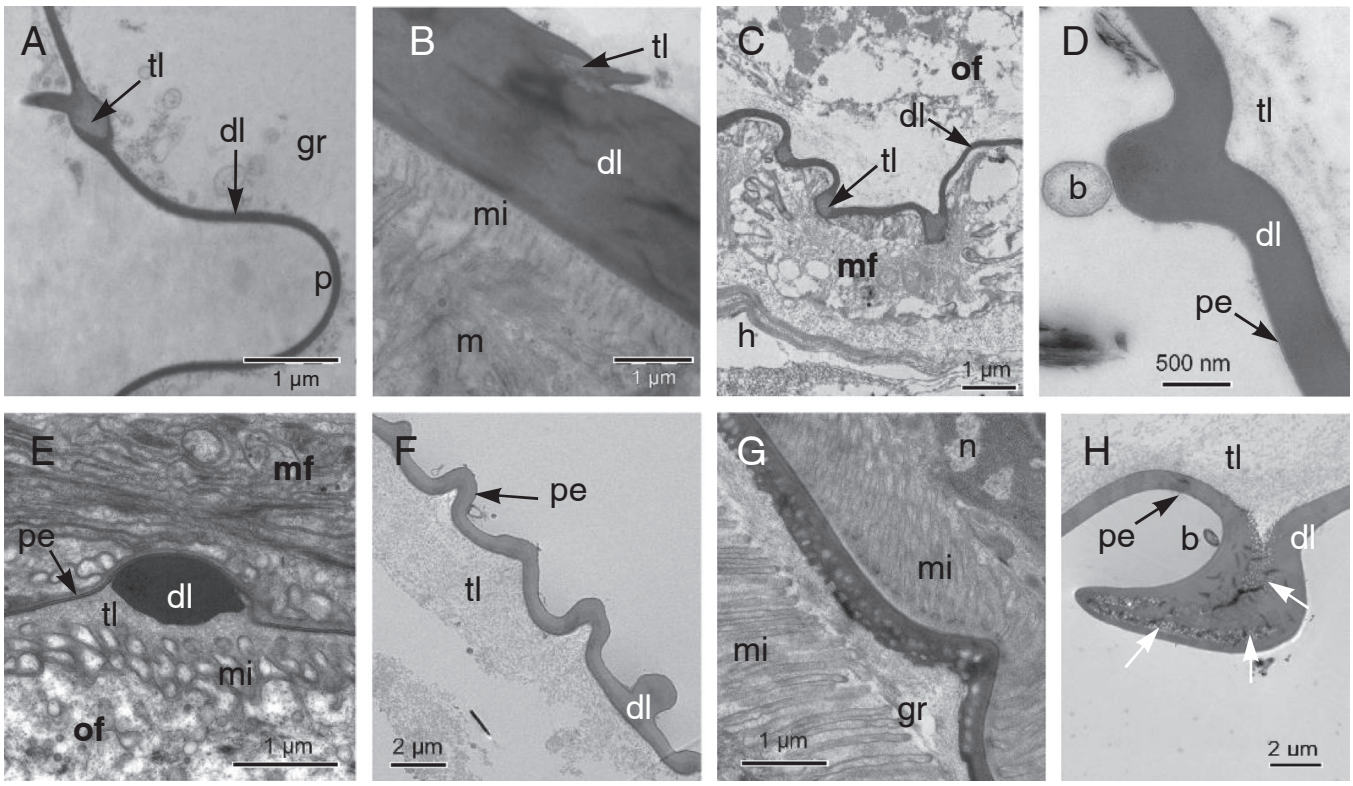

Fig. 10. TEM views on the structure of the periostracum in *Solemya elarraichensis* (A-B); *Saccella commutata* (C-D); *Nuculana soyoae* (E-F) and *Acila insignis* (G-H). A. *Solemya elarraichensis*, periostracum inside the periostracal groove showing a fold with a translucent pouch. B. *S. elarraichensis*, periostracum out of the periostracal groove showing a pouch of translucent secretion at the base of a fold. C. *Saccella commutata*, periostracum in the periostracal groove showing pouches of translucent secretion under each fold. D. *S. commutata,* free periostracum with continuous dark layer. E. *Nuculana soyoae*, dense dark formation under each fold inside the periostracal groove. F. *N. soyoae*, free periostracum with continuous dark layer. G. *Acila insignis,* periostracum with vesicles of translucent secretion at the bottom of the periostracal groove. H. *A. insignis*, free periostracum with some vesicles of translucent secretion (white arrows) inside and under a periostracal fold. b: bacteria; dl: dark layer; gr: periostracal groove; h: blood sinus; m: mantle; mf: middle fold; mi: microvilli; of: outer fold; p: periostracum; pe: pellicle of the periostracum; tl: translucent secretion by the outer fold.

formation of the radial ribs. It is interesting to see in the inter-crenulations the disordered orientation of the prisms formed by the outer side of the OF (Fig. 12C,F) that seem to be secreted without strong cellular control. A model for the formation of the crenulations has been elaborated (Fig. 12G,H), according to which in the crenulation the second outer fold is slightly projected toward the internal shell layer to function as a template for the crenulation.

Bevelander and Nakahara (1966) demonstrated differential absorption from the extrapallial space by the outer surface of the mantle of *Macrocallista maculata.* The micropinocytic vesicles formed under the microvilli gave rise to large vacuoles and lysosomes. According to these authors, the significance of this activity awaits further study. However, in our study, we only observed secretion (glandular or by vesicles through the microvilli) from the mantle epithelium toward the extrapallial space.

Intense metabolic activity has been, however, observed inside the groove between the MF and IF and along the inner epithelium of the IF, where intense secretion of glycocalix has been observed in all the species, together with endocytosis of particles through the apical surface of the cells, the presence of lysosomes in the apical cytoplasms, the presence of large Golgi vesicles along the intercellular spaces and the presence of high amount of glycogen-like granules in their cytoplasm. The presence of numerous lysosomes near the apical surface of the epithelial cells is more conspicuous in nuculanids, particularly in *Nuculana soyoae*. All the above is rather similar to that found in the digestive epithelial absorptive cells of molluscs (Lobo-da-Cunha, 2019) and points to a possible additional feeding function of the inner epithelium of the MF and all the IF in protobranchs. In addition, the presence of large blood sinuses inside the three mantle folds and mantle, with abundance of granulocytes (Fig. 2) would confirm active transport of particles by the granulocytes through the blood spaces. From the inner side of the IF towards the inner pallial epithelium of the mantle, there is an extensive ciliated area in all the protobranchs, whose main function is to control the water flow through the pallial cavity. Audino and Marian (2018) consider these ciliated areas as sensorial in Arcoida, but our observations indicate that the capture of particles may be another main function.

Our study shows that *Solemya elarraichensis*, a chemosymbiotic species (Oliver et al., 2011; Rodrigues et al., 2013), also houses bacteriocytes in the inner epithelium of the MF, together with active secretion of glycocalix and the presence of endocytosis. The middle mantle fold of bivalves is considered the sensorial one, due to the presence of eyes or tentacles, like those present in Pteriomorphia or *Tridacna* spp (Yonge, 1953). However, in *Tridacna*, the middle mantle fold of the siphonal region is greatly enlarged (Yonge, 1953) with the presence of symbiotic zooxanthellae that help in the nutrition of these giant bivalves (Muscatine, 1967). On the other hand, the presence of bacteriocytes in chemosymbiotic bivalves, including *Solemya*, has been experimentally related to a percentage of their nutritional requirements (Le Pennec et al., 1995; Stewart and Cavanaugh, 2006). All the above seem to be compatible with a possible feeding role of the mantle edge, mainly the MF, in this species.

Sensorial cells are present in the MF, some of them without cilia but with a depressed microvillous membrane. Studies on epidermal sensory receptors in molluscs have been mainly focused on recognizable sensory organs such as osphradia, rhinophores, olfactory organs, statocists and

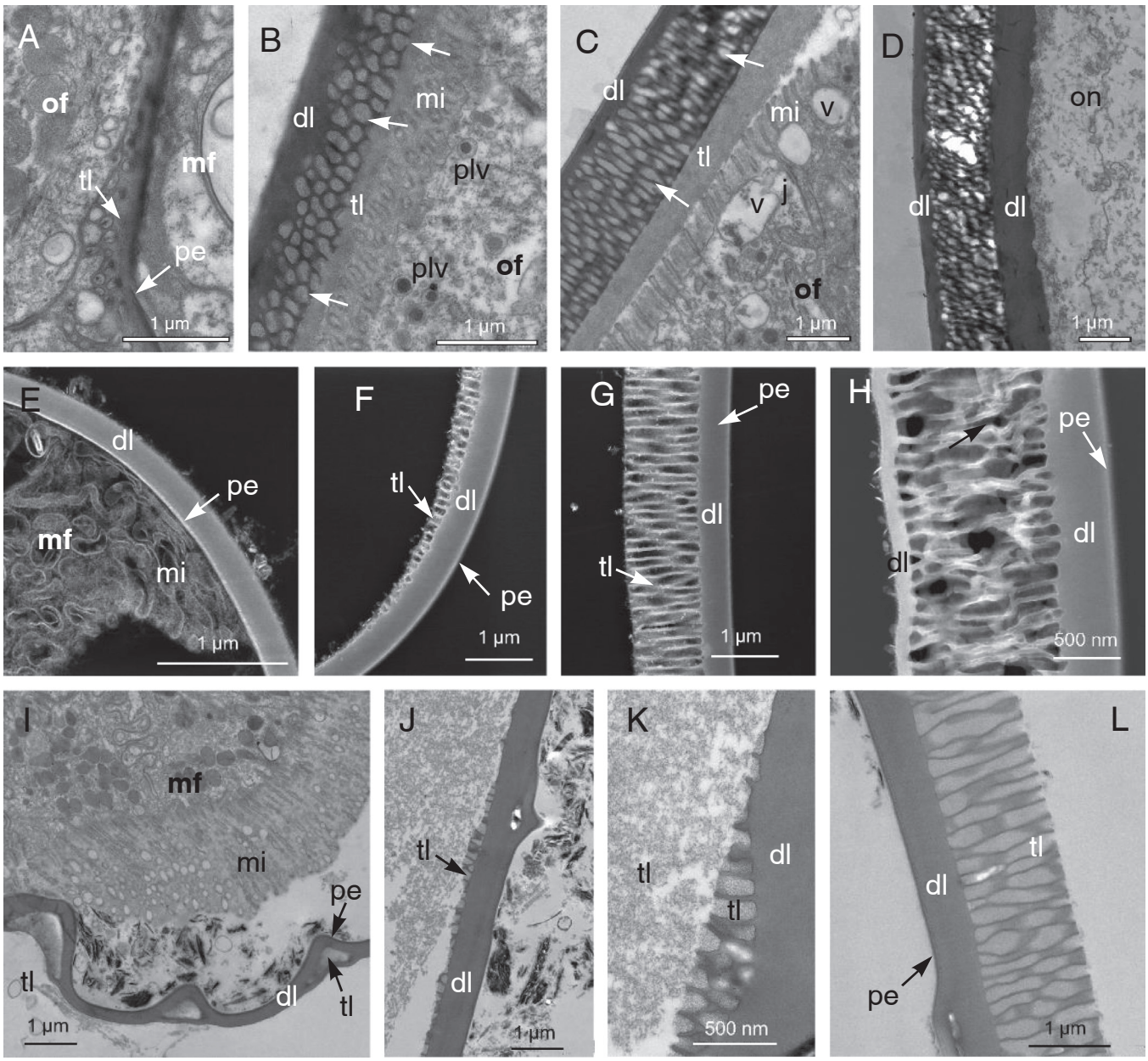

Fig. 11. TEM views of the vesicular periostracum in *Nucula hanleyi* (A-D), TEM-STEM views of periostracum in *Ennucula aegeensis* (E-H) and TEM views of periostracum in *Sarepta speciosa* (I-L). A. Periostracum with some vesicles of translucent secretion (white arrows) at the bottom of the periostracal groove. B. Growth of the vesicles to form a vesicular layer inside the periostracal groove (white arrows). C. The vesicular layer (white arrow) begins to be sealed at the end of the periostracal groove by sclerotization of the translucent layer. D. Periostracum joined with the shell by the dark layer, which seals the vesicular layer (white arrow). E. Periostracum leaving the periostracal groove. F. Free periostracum with the beginning of the vesicular layer. G. Free periostracum with elongate vesicular layer. H. Free periostracum with sealed vesicular layer. I. Periostracum at the end of the periostracal groove with pouches of translucent layer under folds. J,K. Free periostracum showed the growth of the vesicular layer. L. Free periostracum showing a continuous and elongate vesicular layer before being sealed by another dark layer. dl: dark layer; f: outer fold; j: adherens junction; p: periostracum; pe: pellicle of the periostracum; tl: translucent secretion by the outer fold; va: vacuole.

eyes (Bubel et al., 1984; Zardus, 2002). Epidermal sensory perception takes place in molluscs mainly by means of primary receptor cells, most of them ciliate cells. However, non-ciliated sensory cells (microvillous sensory cells), considered as chemosensory, have been found in the general epidermis and in the cephalic tentacles of several pulmonate gastropods, such as *Helix pomatia or Biomphalaria pfeifferi,* among others (Bubel et al., 1984). The sensorial microvillous cells observed in some protobranchs had nervous fibers and glial cells near the basal membrane. The so-called glial cells have been described in many invertebrates that retain nerve elements in the integument, such as molluscs (Nicaise, 1973), flatworms (Bisereva, 2008) or phoronids (Temereva and Malakhov, 2009). The glial cells are characterized by the presence of electron-dense granules in their cytoplasm and are located in the basal epithelium, near the fibers of the nerve plexus, which they can surround partially or entirely.

We have also observed in *Solemya elarraichensis* the section of a tubular gland between the IF and MF, which seems to secrete an oily substance. Yonge (1939) indicated the presence of lubricant mucous glands in the middle fold of *Solemya togata*, and Beedham and Owen (1964) observed in *Solemya parkinsonii* the presence of numerous simple tubular glands, which open to the exterior in the groove between the inner and middle folds secreting a lipo-protein mucous substance. Yonge (1939) suggested that the secretion of these tubular glands possibly functions to lubricate the ventral region of the shell and may be

Table 3
Main characteristics of the mantle edge in Protobranchia. OF: outer mantle fold; MF: middle mantle fold; IF: inner mantle fold.

Species	Mantle folds	OF function	MF function	IF function	Basal Cells	Periostracal layers	Translucent pouches in periostracum
S. elarraichensis	3	shell secretion	sensorial/ feeding	water flux	2	3	yes
N. nucleus	4	shell secretion	sensorial	water flux/uptake particles	2	3	no
N. hanleyi	4	shell secretion	sensorial	water flux/uptake particles	2	3	yes
N. sulcata	4	shell secretion	sensorial	water flux/uptake particles	2	3	no
E. aegeensis	3	shell secretion	sensorial	water flux/uptake particles	2	3	yes
A. insignis	3	shell secretion	sensorial	water flux/uptake particles	2	3	yes
L. pella	3	shell secretion	sensorial	water flux/uptake particles	2	3	no
N. soyoae	3	shell secretion	sensorial	water flux/uptake particles	2	3	no
S. commutata	3	shell secretion	sensorial	water flux/uptake particles	2	3	yes
S. speciosa	3	shell secretion	sensorial	water flux/uptake particles	2	3	yes

responsible for the water-repellent nature of the periostracum; but probably could also be involved in consolidating the muddy substrate around the animal.

One remarkable feature of the protobranch mantle folds is their flexibility and ability for some degree of plication, which seem to be used for different purposes. The OF folding could be related to an increase in the potential for periostracum secretion, particularly in *E. aegeensis* as a way to increase the extent of secretory mantle epithelium. The MF folding seems to be related to the guiding of the periostracum toward the outer shell surface.

The IF folding could be related to sediment retention for preventing pallial cavity clogging. However, in protobranchs, part of the exogenous material will be trapped by the glycocalix secreted by the pallial side epithelium, before the particles are taken up by pinocitic vesicles, most of which are transported by the intercellular zones.

Acid mucopolysaccharide and acid glycoprotein are known to cause red and purple metachromasia respectively with toluidine blue stain. Green metachromasia by toluidine blue has been reported, among other instances, in the organic cups of the solenogaster *Proneomenia aglaopheniae* and inner cuticle of the chiton *Acanthochitona crinitus* (Beedham and Trueman, 1968) or in the outer mantle fold of *Neotrigonia margaritacea* (Checa et al., 2014). The presence of phenolic mucopolysaccharide complexes in the epithelial cells of the outer mantle fold of *N. margaritacea* was related by these authors to a more intense hardening of the periostracum. The brownish metachromasia is usually related to the presence of sulfatide and acidic lipids (Sridharan and Shankar, 2012). The intense green metachromasia of the mantle edges and foot epithelial layers of a methacrylate embedded specimen of *Nucula sulcata* fixed with formaldehyde and stained with Toluidine blue (pH 8,3) could be related to the presence of high levels of diphenols for faster and stronger tanning of the translucent layer. The periostracum in this species is very thick and tanned. On the other hand, the brownish and yellowish metachromasia inside the mantle could be then associated with the high level of sulfur in the environment that could favor the presence of sulfated glycoproteins and sulfated mucopolysaccharides in the tissues (Sridharan and Shankar, 2012). However, semithin sections of *N. sulcata* and *S. elarraichensis* which live in reduced environment with high amount of sulfur, do not show green metachromasia. Probably the small size of the pieces used for TEM and the different protocols influence the differences.

4.2. Formation and structure of the periostracum

The presence of two basal cells and a three-layered periostracum is the general and common pattern found in the studied protobranchs. One basal cell is the general pattern in Bivalves (Checa and Salas, 2017). The latter corresponds to the first cell, or two first cells in protobranchs, of the OF inner side and it is the only responsible for the secretion of the nanometric pellicle because this layer maintains its initial thickness along the periostracum in all the studied bivalves (Salas et al., 2012; Checa and Salas, 2017). The presence of two basal cells in all the studied protobranchs supports the monophyly of this clade, like some molecular studies indicate (Kocot et al., 2011; Smith et al., 2011; Sharma et al., 2012, 2013).

The very incurved MF epithelium at the bottom of the periostracal groove that pushes the basal cells toward the middle of the OF, together with a long free periostracum, found in nuculids, resembles those found in *Neotrigonia maragaritacea* (Checa et al., 2014) or *Cardium (=Cerastoderma) edule* (Richardson et al., 1981) and *Glycymeris* (obser. pers. C. Salas). All the latter seem to be adapted to epibenthic, shallow burrowing life, in which frequent strong movements of the valves for expulsion of the feces or escaping from predators is common (Yonge, 1939), which could break the forming periostracum. The nuculanids, with less incurved MF, have siphons and their movements are less strong and less frequent (Yonge, 1939). The strong digitate cell membranes together with the strong adherens junctions observed between adjacent epithelial cells from the margin folds could be also related to the frequent movements of the mantle edge in these shallow burrowing species. Finally, *Solemya*, a very deep burrowing species which is able to remain for days without any signal of movement (Yonge, 1939), has its basal cells practically at the bottom of the periostracal groove and there are not interdigitate intercellular membranes between adjacent epithelial cell from the mantle folds.

The periostracum of *S. togata* shows in the paraffin sections three differentiated layers under trichromic VOF stain (Fig. 3A), a fine external orange layer, a middle green layer and a large internal red layer. The orange color could be related to the presence of polyphenols; the green color could be due to the presence of abundant collagen fibers and the red color in tissues is related to muscular elastic fibers, but in the periostracum could be related to another type of elastic collagen. All this amount of collagen fibers in the periostracum could be related to the capacity of *Solemya* to extend very far the mantle and its associated periostracum (Beedham and Owen, 1965; Yonge, 1939).

According to Bubel (1973), the pellicle is absent in *N. sulcata,* which

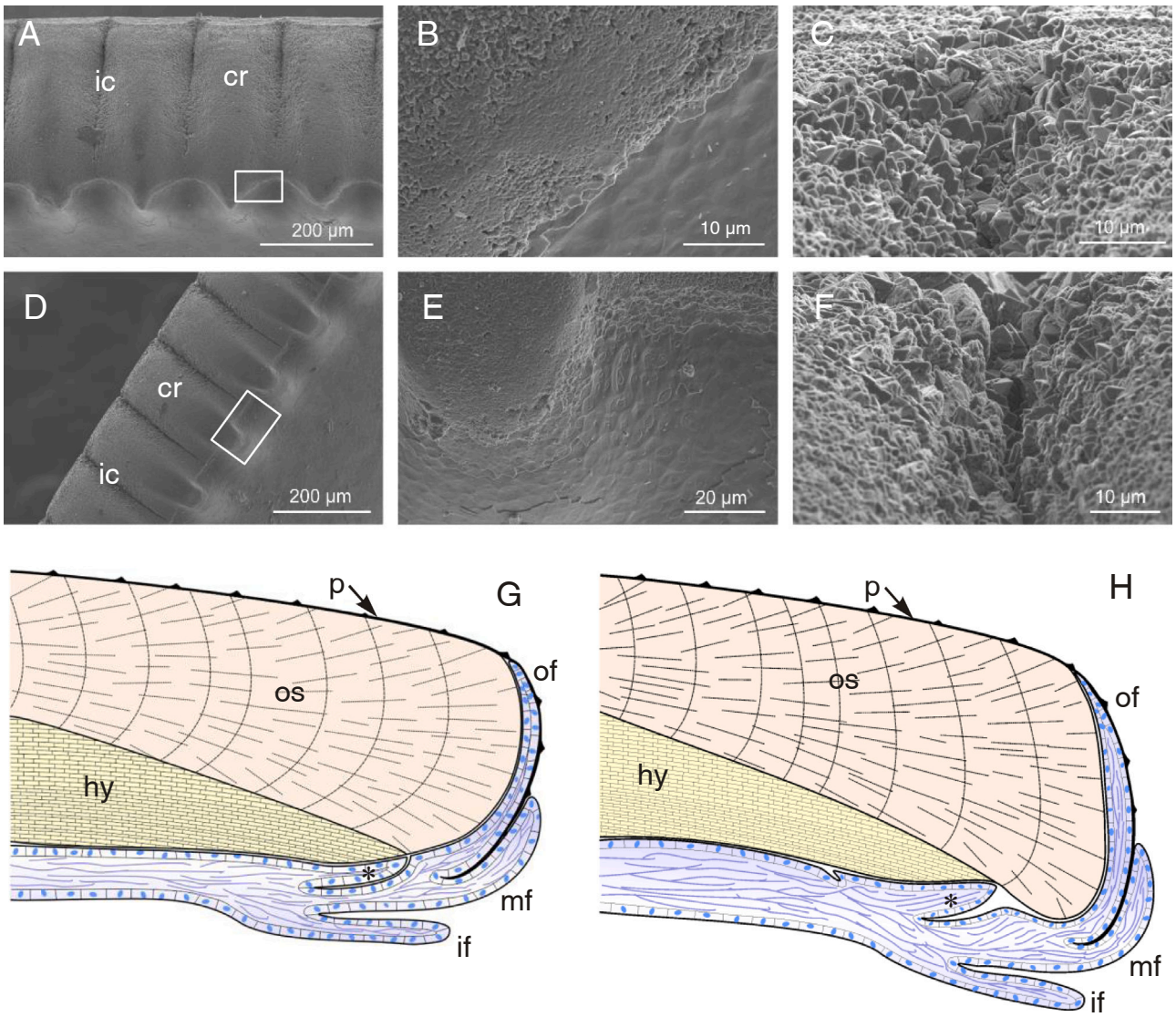

Fig. 12. FESEM views of the internal margin of the shell of *Nucula nucleus* (A-C) and *Nucula hanleyi* (D-F). A-D. Views of the crenulations at the margin of the valves. B,E. Detail of the white frame of A and D, showing the nacre layer at the crenulation zones. C,F. Views of the prisms in the inter-crenulations zones. G. Model of formation of the shell margin at the inter-crenulation zone. The second outer fold is appressed on the OF. H. Model of formation of the shell margin at the crenulation zone. The second outer fold (asterisk) is visible and slightly projected toward the internal side of the shell. cr: crenulation; hy: hypostracum; ic: inter-crenulation zone; if: inner fold; mf: middle fold; of: outer fold; os: ostracum; p: periostracum.

he considered the primitive condition of the nuculids. However, our electron microscopic observations of *N. sulcata, N. nucleus, A. insignis* and *E. aegeensis* confirm the presence of a pellicle layer. It is ill-defined in some of them, probably due to the strong polymerization of the dark layer, which in protobranchs becomes as dark as the pellicle, e.g. in *N. sulcata* and *N. nucleus*.

The formation of pouches of translucent layer within the dark layer seems to be a periostracal characteristic of most of the protobranchs with folded periostracum, such as *S. commutata*, *A. insignis* or *S. elarraichensis*. There is a continuous vesicular layer in the periostracum of *N. hanleyi, E. aegeensis* and *Sarepta speciosa*. The formation of this vesicular layer in the free periostracum in *E. aegeensis* and *S. speciosa* would be related to a high elasticity of the OF, which would secrete TL underneath the free periostracal dark layer, probably by the distal margin. These species live in sandy or muddy bioclastic bottoms with strong currents, where a vesicular periostracum could cushion frictions from the bioclasts. In *Nuculana soyoae* the pouches of translucent layer penetrate the scales or projections of the periostracum while in *Saccella*, *Lembulus* and *Solemya* there are few or only one vesicle respectively within each periostracal fold. The function of the vesicles under the folds would be related to a high flexibility. In the case of *S. elarraichensis*, although the animal is very sedentary, the mantle edge and the overlying periostracum is very broad and elastic (hence their name of "awning clams"). The continuous DL found in *N. sulcata, N. nucleus,* and *Lembulus pella*, without any TL pouch inside the dark layer, would be related with a more sedentary life, but could also confirm the non-monophyly of most nuculids and nuculanid genera and families showed by molecular studies (Sharma et al., 2013; Bieler et al., 2014; Combosch et al., 2017; Sato et al., 2020) and shell microstructure (Sato and Sasaki, 2015; Sato et al., 2017).

The periostracum in *Sarepta speciosa* shows characteristics found in both orders (Nuculida and Nuculanida). Inside the periostracal groove the dark layer encloses a vesicle of translucent layer within each periostracal fold, like in *S. commutata* (Nuculanidae), but when leaving the periostracal groove, the translucent layer begins to form more vesicles under each periostracal fold, like in the nuculid *A. insignis*, and finally the free periostracum has a continuous vesicular structure, very similar to that found in *N. hanleyi* or *E. aegeensis*. The coexistence of periostracal

characteristics from both clades (Nuculida and Nuculanida) in *Sarepta speciosa* could either indicate an intermediate or basal position for Sareptidae, or alternatively be an environmentally controlled trait. On the other hand, the morphology of the mantle edge in *Sarepta speciosa* resembles that of other nuculanids, in which the inner mantle fold is long and flexible, able to manage the capture and absorption of detritus. In addition, the interior of the shell is not nacreous, a character state proper of Nuculanidae. The molecular studies carried out with specimens included in Sareptidae, such as *Pristigloma nitens*, *P. alba* (Sharma et al., 2013; Combosch et al., 2017) and *Sarepta speciosa* (Sato et al., 2020) unite phylogenetically this group within Nuculanida, but according to the latter as superfamily Sareptoidea.

Funding

This research was funded by the projects CGL2017-85118-P and PID2020-116660GB-I00 of the Spanish Ministry of Economy, Industry and Competitiveness. Funding for open access charge has been provided by the University of Málaga/CBUA.

Declaration of Competing Interest

The authors declare that they have no known competing financial interests or personal relationships that could have appeared to influence the work reported in this paper.

Acknowledgments

We are particularly grateful to Kei Sato (The University Museum, The University of Tokyo, Tokyo, Japan) for the collection of specimens of *Acila insignis*, *Nuculana soyoae* and *Sarepta speciosa* in Japan and for the pictures of the Japanese species. We would like to thank José Luis Rueda (Spanish Institute of Oceanography) and the crew of the CHICA (INDEMARES) cruise in the Gulf of Cádiz for the capture of specimens of *Solemya elarraichensis* and Cristina García and the crew of MEDITS cruise for the capture of specimens of *Nucula sulcata.* We thank Eva M. Jiménez Enjuto (BIONAND: Andalusian Centre of Nanomedicine and Biotechnology, Málaga) for the methacrylate embedding and sectioning of the specimens of *Nucula nucleus*, *Nucula sulcata* and *Saccella commutata*. Thanks to Adolfo Martínez, technician of the University of Malaga of the TEM-STEM FEI Talos 200X and Gregorio Martín Caballero technician of the University of Malaga of the Scanning Electron Microscopic service. We are grateful to Serge Gofas for help with mounting the plates.

References

Allen, J.A., Sanders, H.L., 1996. The zoogeography, diversity and origin of the deep sea protobranch bivalves of the Atlantic: the epilogue. Prog. Oceanogr. 38, 95–153.
Ansell, A.D., 1961. The functional morphology of the British species of Veneracea (Eulamellibranchia). J. Mar. Biol. Assoc. 41, 489–517.
Audino, J.A., Marian, J.E.A., 2016. On the evolutionary significance of the mantle margin in pteriomorphian bivalves. Am. Malacol. Bull. 34, 148–159.
Audino, J.A., Marian, J.E.A., 2018. Comparative and functional anatomy of the mantle margin in ark clams and their relatives (Bivalvia: Arcoidea) supports association between morphology and life habits. J. Zool. 305, 149–162.
Audino, J.A., Marian, J.E.A., Wanninger, A., Lopes, S.G., 2015. Mantle margin morphogenesis in *Nodipecten nodosus* (Mollusca: Bivalvia): new insights into the development and the roles of bivalve pallial folds. BMC Dev. Biol. 15, 22.
Audino, J.A., Serb, J.M., Marian, J.E.A., 2020. Phylogeny and anatomy of marine mussels (Bivalvia: Mytilidae) reveal convergent evolution of siphon traits. Zool. J. Linn. Soc. 190, 592–612.
Beedham, G.E., Owen, G., 1965. The mantle and shell of *Solemya parkinsoni* (Protobranchia: Bivalvia). J. Zool. 145, 405–430.
Beedham, G.E., Trueman, E.R., 1968. The cuticle of the Aplacophora and its evolutionary significance in the Mollusca. J. Zool. 154, 443–451.
Bevelander, G., Nakahara, H., 1966. Correlation of lysosomal activity and ingestion by the mantle epithelium. Biol. Bull. 131, 76–82.
Bieler, R., Carter, J.G., Coan, E.V., 2010. Classification of Bivalve families. Pp. 113-133, in: Bouchet, P. & Rocroi, J.P. Nomenclator of Bivalve Families. Malacologia 52, 1–184.
Bieler, R., Mikkelsen, P.M., Collins, T.M., Glover, E.A., González, V.L., Graf, D.L., Harper, E.M., Healy, J., et al., 2014. Investigating the Bivalve Tree of Life – an exemplar-based approach combining molecular and novel morphological characters. Invert. Syst. 32–115.
Bisereva, N.M., 2008. Ultrastructure of glial cells in the nervous system of *Grillotia erinaceus*. Cell Tissue Biol. 2, 251–264.
Bubel, 1984. Mollusca. Chapter 24. Epidermal cells. In: Bereiter-Hahn, J., Matoltsy, A.G., Richards, K.S. (Eds.), Biology of the Integument: Invertebrates. Springer, New York, pp. 400–485.
Bubel, A., 1973. An electron-microscope study of periostracum formation in some marine bivalves. I. The origin of the periostracum. Mar. Biol. 20, 213–221.
Checa, A., Salas, C., 2017. Periostracum and Shell formation in the Bivalvia. Treatise Online, part N, Revised, Vol. 1, Chap. 3. Kansas University Paleontological Institute, pp. 1–51.
Checa, A.G., Jiménez-Jiménez, A.P., 2003. Rib fabrication in Ostreoidea and Plicatuloidea (Bivalvia, Pteriomorphia) and its evolutionary significance. Zoomorphology 122, 145–159.
Checa, A.G., Salas, C., Harper, E.M., Bueno-Pérez, Jd.D., 2014. Early stage biomineralization in the periostracum of the 'living fossil' bivalve *Neotrigonia*. PLoS One 9, e90033.
Combosch, D.J., Collins, T.M., Glover, E.A., Graf, D.L., Harper, E.M., Healy, J.M., Taylor, J.D., 2017. A family-level tree of life for bivalves based on a Sanger-sequencing approach. Mol. Phylogenet. Evol. 107, 191–208.
Davenport, J., 1988. The feeding mechanism of *Yoldia* (=*Aequiyoldia*) *eightsi* (Courthouy). Proc. R. Soc. Lond. Ser. B 1269, 431–442.
Etter, R.J., Rex, M.A., Chase, M.R., Quattro, J.M., 2005. Population differentiation decreases with depth in deep-sea bivalves. Evolution 59, 1479–1491.
Etter, R.J., Boyle, E.E., Glazier, A., Jennings, R.M., Dutra, E., Chase, M.R., 2011. Phylogeography of a pan-Atlantic abyssal protobranch bivalve: implications for evolution in the Deep Atlantic. Mol. Ecol. 20, 829–843.
García-Gasca, S., García-Domínguez, F., 1995. Histología comparada del manto marginal y paleal de las almejas *Megapitaria aurantiaca* (Sowerby, 1831) y *M. squalida* (Sowerby, 1835) (Bivalvia: Veneridae). An. Esc. Nac. Cienc. Biol. México 40, 173–181.
Gofas, S., Salas, C., 1996. Small Nuculidae (Bivalvia) with functional primary hinge in the adults. J. Conchol. 35, 427–436.
Gutiérrez, M., 1967. Coloración histológica para ovarios de peces, crustáceos y moluscos. Investig. Pesq. 32, 265–271.
Hillman, R.E., Shuster, C.N., 1966. A comment on the origin of the fourth fold in the mantle of the Quahog, *Mercenaria mercenaria*. Chesap. Sci. 7, 112–113.
Jennings, R.M., Etter, R.J., Ficarra, L., 2013. Population differentiation and species formation in the deep sea: the potential role of environmental gradients and depth. PLoS ONE 8, e77594. https://doi.org/10.1371/journal.pone.0077594.
Kocot, K.M., Cannon, J.T., Todt, C., Citarella, M.R., Kohn, A.B., Meyer, A., Santos, S.R., Schander, C., Moroz, L.L., Lieb, B., Halanych, K.M., 2011. Phylogenomics reveals deep molluscan relationships. Nature 477, 452–456.
Le Pennec, M., Beninger, P.G., Herry, A., 1995. Feeding and digestive adaptation of bivalve molluscs to suphide-rich habitats. Comp. Biochem. Physiol. A Physiol. 111 (2), 183–189.
Lemer, S., Bieler, R., Giribet, G., 2019. Resolving the relationships of clams and cockles: dense transcriptome sampling drastically improves the bivalve tree of life. Proc. R. Soc. B 286 (1896), 20182684.
Lobo-da-Cunha, A., 2019. Structure and function of the digestive system in molluscs. Cell Tissue Res. 377, 475–503.
Morse, M.P., Zardus, J.D., 1997. Bivalvia. In: Harrison, F.W., Kohn, A.J. (Eds.), Microscopic Anatomy of Invertebrates, 6. Wiley & Sons, pp. 7–118.
Morton, B., 2012. The biology and functional morphology of *Nucula pusilla* (Bivalvia: Protobranchia: Nuculidae) from Western Australia, Australia: primitive or miniature simplicity? Rec. W. Aus. Mus. 27, 85–100.
Morton, B., Peharda, M., 2008. The biology and functional morphology of *Arca noae* (Bivalvia: Arcidae) from the Adriatic Sea, Croatia, with a discussion on the evolution of the bivalve mantle margin. Acta Zool. 89, 19–28.
Muscatine, L., 1967. Glycerol excretion by symbiotic alga from corals and *Tridacna* and its control by the host. Science 156, 516–519.
Nicaise, G., 1073. The gliointerstitial system of Mollusca. Int. Rev. Cytol., 34, pp. 251–332.
Oliver, G., Rodrigues, C.F., Cunha, M.R., 2011. Chemosymbiotic bivalves from the mud volcanoes of the Gulf of Cadiz, NE Atlantic, with descriptions of new species of Solemyidae, Lucinidae and Vesicomyidae. ZooKeys 113, 1.
Pelseneer, P., 1891. Contribution à l'étude des Lamellibranches. Arch. Biol. 11, 147–312 pl. 6-23.
Ponder, W.F., Lindberg, D.R., Ponder, J.M., 2019. Biology and Evolution of the Mollusca. CRC Press, p. 924 (xxi +).
Quayle, D.B., 1952. Structure and biology of the larva and spat of *Venerupis pullastra* (Montagu). Trans. R. Soc. Edinb. 62, 255–297.
Richardson, C.A., Runham, N.W., Crisp, D.J., 1981. A histological and ultrastructural study of the cells of the mantle edge of a marine bivalve, *Cerastoderma edule*. Tissue Cell 13, 715–730.
Rodrigues, C.F., Hilário, A., Cunha, M.R., 2013. Chemosymbiotic species from the Gulf of Cadiz (NE Atlantic): distribution, life styles and nutritional patterns. Biogeoscience 10, 2569–2581.
Salas, C., Marina, P., Checa, A.G., Rueda, J.L., 2012. The periostracum of *Digitaria digitaria* (Bivalvia: Astartidae): formation and structure. J. Molluscan Stud. 78, 34–43.
Sato, K., Sasaki, T., 2015. Shell microstructure of Protobranchia (Mollusca: Bivalvia): diversity, new microstructures and systematic implications. Malacologia 59, 45–103.

Sato, K., Checa, A.G., Rodríguez-Navarro, A.B., Sasaki, T., 2017. Crystallographic texture analysis of Protobranchia (Mollusca: Bivalvia): interspecific variations, homology and shell microstructural evolution. J. Molluscan Stud. 83, 304–315.
Sato, K., Kano, Y., Setiamarga, D.H.E., Watanabe, H.K., Sasaki, T., 2020. Molecular phylogeny of protobranch bivalves and systematic implications of their shell microstructure. Zool. Scr. 49, 458–472.
Schaefer, K., 2000. The adoral sense organ in protobranch bivalves (Mollusca): comparative fine structure with special reference to *Nucula nucleus*. Invert. Biol. 119, 188–214.
Sharma, P.P., González, V.L., Kawauchi, G.Y., Andrade, S.C., Guzmán, A., Collins, T.M., Glover, E.A., Harper, E.M., Healy, J.M., Mikkelsen, P.M., Taylor, J.D., Bieler, R., Giribet, G., 2012. Phylogenetic analysis of four nuclear protein-encoding genes largely corroborates the traditional classification of Bivalvia (Mollusca). Mol. Phylogenet. Evol. 65, 64–74.
Sharma, P.P., Zardus, J.D., Boyle, E.E., González, V.L., Jennings, R.M., Mcintyre, E., Wheeler, W.C., Etter, R.J., Giribet, G., 2013. Into the deep: a phylogenetic approach to the bivalve subclass Protobranchia. Mol. Phylogenet. Evol. 69, 188–204.
Simone, L.R.L., 2009. Comparative morphology among representatives of main taxa of Scaphopoda and basal protobranch Bivalvia (Mollusca). Pap. Avuls. Zool. 49, 405–457.
Smith, S.A., Wilson, N.G., Goetz, F.E., Feehery, C., Andrade, S.C.S., Rouse, G.W., Giribet, G., Dunn, C.W., 2011. Resolving the evolutionary relationships of molluscs with phylogenomic tools. Nature 480, 364–367.
Sridharan, G., Shankar, A.A., 2012. Toluidine blue: a review of its chemistry and clinical utility. J. Oral Maxillofac. Pathol. 16, 251–255.
Stasek, C.R., 2009. The ciliation and function of the labial palps of *Acila castrensis* (Protobranchia, Nuculidae). J. Zool. 137, 511–538.
Stasek, C.R., McWilliams, W.R., 1973. The comparative morphology and evolution of the molluscan mantle edge. Veliger 16, 1–19.
Stewart, F.J., Cavanaugh, C.M., 2006. Bacterial endosymbioses in *Solemya* (Mollusca: Bivalvia)-model systems for studies of symbiont-host adaptation. Antonie Van Leeuwenhoek 90, 343–360.
Stone, H.M.I., 1998. The Functional Morphology and Evolution of Pronounced Shell Ornament in Epifaunal Bivalves. Cambridge University, Cambridge, pp. 1–271 (Unpublished Ph.D. thesis).
Temereva, E.N., Malakhov, V.V., 2009. Microscopic anatomy and ultrastructure of the nervous system of *Phoronopsis harmeri* Pixell, 1912 (Lophophorata: Phoronida). Russ. J. Mar. Biol. 35, 388–404.
Waller, T.R., 1978. Morphology, morphoclines and a new classification of the Pteriomorphia (Mollusca: Bivalvia). Philos. Trans. R. Soc. Lond. B 284, 345–365.
WoRMS, 2022. Protobranchia. Accessed through: World Register of Marine Species at: ⟨https://www.marinespecies.org/aphia.php?p=taxdetails&id=106⟩ on 2022-05-01. ⟨DOI: 10.14284/170⟩.
Yonge, C.M., 1939. The protobranchiate Mollusca; a functional interpretation of their structure and evolution. Philos. Trans. R. Soc. Lond. B 230, 79–148.
Yonge, C.M., 1953. Mantle chambers and water circulation in the Tridacnidae (Mollusca). Proc. Zool. Soc. Lond. 123, 551–561.
Yonge, C.M., 1957. Mantle fusions in the Lamellibranchia. Pubbl. Staz. Zool. Napoli 29, 151–171.
Yonge, C.M., 1983. Symmetries and the role of the mantle margins in the bivalve Mollusca. Malacol. Rev. 16, 1–10.
Zardus, J.D., 2002. Protobranch bivalves. Adv. Mar. Biol. 42, 1–65.
Zardus, J.D., Morse, M.P., 1998. Morphology and ultrastructure of the pericalymma larva of *Acila castrensis* (Bivalvia: Protobranchia: Nuculoida). Invert. Biol. 117, 221–244.
Zardus, J.D., Etter, R.J., Chase, M.R., Rex, M.A., Boyle, E.E., 2006. Bathymetric and geographic population structure in the pan-Atlantic deep-sea bivalve *Deminucula atacellana* (Schenck, 1939). Mol. Ecol. 15, 639–651.